Journal of African Earth Sciences 224 (2025) 105533

Contents lists available at ScienceDirect

Journal of African Earth Sciences

journal homepage: www.elsevier.com/locate/jafrearsci

Hydrogeochemical and hydrogeological baseline study following the mining of asbestos at the Havelock Mine, Bulembu, eSwatini

Christian Wolkersdorfer[a,*], Kagiso S. More[a,d], Elke Mugova[a], Nokuthula Nchabeleng[b], Anna Johanna Sotiralis[c]

[a] *SARChI Chair for Mine Water Management, Department of Environmental, Water and Earth Sciences, Tshwane University of Technology, Private Bag X680, Pretoria, 0001, South Africa*

[b] *Sustainable Environment and Water Utilization Processes, Department of Chemical Engineering, University of Pretoria, Private Bag X20, Hatfield, 0028, South Africa*

[c] *91 7th Street, Menlo Park, 0081, South Africa*

[d] *Now: University of South Africa, Private Bag X6, Science Campus, Florida, Johannesburg, 1709, South Africa*

ARTICLE INFO

Handling Editor: M Mapeo

Keywords:
Chrysotile asbestos
eSwatini
Hydrogeochemistry
Abandoned underground mine

ABSTRACT

This study examined the hydrogeological and hydrochemical conditions around Bulembu, eSwatini, two decades post-closure of the Havelock asbestos mine. On-site parameters and water samples underwent chemical and stable isotope analysis, supplemented by flow measurements and tracer tests with NaCl and uranine. Multivariate statistical analysis and PHREEQC modelling identified three water groups: i) low mineralised surface water (32 mg/L TDS), ii) mining-influenced water from the Havelock mine pool (212 mg/L TDS), and iii) tailings seepage water (411 mg/L TDS). All are earth alkaline, hydrogen carbonate-dominant, dominated by Mg and hydrogen carbonate ions. Surface water complies with WHO standards, except for elevated As in the mine pool and Cr in waste rock seepage. Chemical and tracer test results indicate a well-mixed, low-residence-time mine pool. Both the Tutusi river catchment and the upper Nkomazana catchment as well as water courses downstream of the abandoned mine exhibit pristine water quality. The authors propose inclusion of the area in a trans-boundary national park with the Barbeton Makhonjwa Mountains UNESCO World Heritage Site. They recommend amelioration of tailings, not remining, to safeguard the environment and local population from asbestos exposure.

1. Introduction

Following the cessation of tailings processing at the King and Shabanie mines in Zimbabwe (Flanagan, 2023), there are currently no active asbestos mines in Southern Africa. Yet, the remains of abandoned asbestos mines are nevertheless affecting the environment and local communities (Cornelissen et al., 2019), and the existing installations where asbestos was used are still of concern, specifically in these developing countries (Thives et al., 2022). Asbestos refers to a group of mineral fibres including chrysotile, amosite and crocidolite (IARC Working Group on the Evaluation of Carcinogenic Risks to Humans, 2012; Pohl, 2020; Ross, 1999; Vallero and Blight, 2019), whereas chrysotile is considered less of a health hazard when compared to the others (McDermott et al., 1982). One of many examples where the remains of asbestos mining are affecting the local community, is the abandoned Havelock Mine in Bulembu (Hhohho region), on the north-western boarder of eSwatini (formerly Swaziland) to South Africa (Fig. 1). Asbestos mining there was once a major contributor to South African and Swazi mining revenues, reaching more than 90% of the mineral production in Swaziland (Jourdan, 1990; Scott, 1950). In the Pigg's Peek area, the Havelock mine was the main employer (McCulloch and Tweedale, 2008) with up to 3000 miners working on the site (McCulloch, 2005).

The Havelock mine had the world's 4th largest asbestos deposit (Schlüter and Schumann, 2018). In 1939 the mine was opened and operated by Turner & Newall (T&N) of Manchester, first as an open pit mine and from 1948 as an underground mine. Today, Bulembu is a small village with an orphanage for children, with the remains of the mining activities being still very present. Two predominantly unremediated tailings dumps are a dominating feature of the landscape and cause asbestos air pollution (Schlüter and Schumann, 2018) and tailings erosion into the receiving water courses. Mhlanga-Mdluli (2012), using

* Corresponding author.
E-mail addresses: christian@wolkersdorfer.info (C. Wolkersdorfer), moreks@unisa.ac.za (K.S. More), elke.mugova@grubenwasser.org (E. Mugova), nokuthulanzimande23@gmail.com (N. Nchabeleng), anse4444@icloud.com (A.J. Sotiralis).

https://doi.org/10.1016/j.jafrearsci.2024.105533
Received 30 December 2023; Received in revised form 30 June 2024; Accepted 29 December 2024
Available online 30 December 2024
1464-343X/

Fig. 1. Geographical location of the abandoned Havelock asbestos mine in Bulembu, eSwatini.

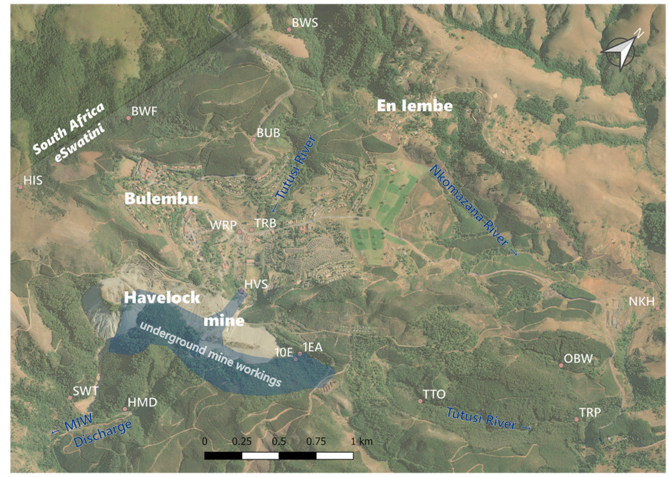

Fig. 2. Sampling locations and geographical details of Bulembu and the abandoned Havelock mine site (Source: Esri, Maxar, Earthstar Geographics, HERE, Garmin, USGS, Intermap, INCREMENT P, NRCan, Esri Japan, METI, Esri China (Hong Kong), Esri Korea, Esri (Thailand), NGCC, © OpenStreetMap contributors, and the GIS User Community). Simplified outline of underground mine workings (transparent blue) from Havelock Asbestos Mines Swaziland Ltd. – Havelock Mine – Underground Plan – Scale 1:500 (Bulembu Mining Museum). (For interpretation of the references to colour in this figure legend, the reader is referred to the Web version of this article.)

a 1997 study by the Ministry of Natural Resources and Energy (Swaziland), reports that discharges from the Havelock mine caused negative effects on the trout population in the Komati River downstream from the mine. Asbestos fibres from these tailings have the potential to be transported by wind or water, which could result in contamination of the local hydrogeological system. It is therefore essential to gain an understanding of the hydrogeochemical conditions in this context in order to assess potential asbestos pollution and its effect on water quality and ecosystem health. Limitations of this study were the underground accessibility of the abandoned mine and the fact that the main vertical shaft is blocked at a depth of 99 m. This prevented continuous measurements of the on-site parameters in the main vertical shaft so far, nor could water samples be taken therein. Consequently, nothing can be said about potential mine water stratification. Yet, for the conclusions about the baseline parameters of the area around the Havelock mine, this is unrelated.

The objective of this study is to address the existing knowledge gap regarding the hydrogeochemical conditions in the area surrounding the Havelock mine. No hydrogeological studies of the area have been carried out or published during the mine's history or since its closure in 2001, and no water quality data are available in the mine's records. This study will therefore provide baseline data on the hydrogeochemical situation around the abandoned Havelock mine and contextualise the results in view of the mine's and the surrounding's geological setting, specifically the Tutusi river catchment area. In addition, the study will provide background information on the health issues associated with asbestos mining and conclude whether the current situation is adversely affecting receiving water courses and potential remediation strategies. All data is based on four sampling campaigns in December 2022, Mai 2023, June 2023 and February 2024.

2. Location and mining history

Bulembu is a former mining town in the north-western part of eSwatini, about 20 km south-southeast of Barberton (South Africa) and 4 km south of eSwatini's highest peak, Emlembe (1862 m). The Havelock open pit and underground mine covered an area of 1.5 × 0.4 km directly south of Bulembu (Fig. 2). Today, the mine wastes in two asbestos tailings dumps and one waste rock pile cover an area of about 50 ha (Fig. 3). Chrysotile (also called white asbestos) mining at Havelock began in 1939. To preserve the mineral's physical properties, asbestos was milled dry, and in conjunction with ore crushing, sorting, milling and bagging (Anonymous, 1978) created a lot of dust on the mine site and in its vicinity. The former residences of Bulembu, which were previously uninhabited, are currently utilized by a Christian organization, Bulembu Ministries, for the purpose of providing shelter to orphaned children (John, 2020).

Fig. 3. Overview of the asbestos tailings at Bulembu, eSwatini on the left of the image and waste rock at the right (sampling location SWT). The buildings in the centre left belong to the former Havelock vertical shaft.

From 1939 to around 1980, the Havelock/Bulembu asbestos mine was owned and managed by the British company T&N, which was the largest employer and taxpayer in Swaziland for several decades, and until 2001 by a consortium between the Havelock Asbestos Mines company and the Government of Swaziland. When T&N declared bankruptcy it thus avoided legal action, compensating 600 Havelock miners and their families, and the cost of clean-up of the mine site (Coakley, 2001). It's worth noting that while some see this typical habit of mining companies transferring assets to small, local companies as a proactive "exit" strategy avoiding issues related to miners and the environment, others might see it as highly unethical (Kazan-Allen, 2003).

Initially, the mine was operated as an opencast mine and, once underground mining started in 1948, also by a three-compartment incline shaft. This inclined shaft was located directly east of the two treatment plants and the rock plant and later was replaced by the vertical shaft as the main mine access. Between 1961 and 1964 the 7 m diameter four-compartment vertical shaft was constructed, which was deepened to 504 m below shaft collar in the early 1970ies (Anonymous, 1978; Barton, 1986). When it was decommissioned in 2001, it was serving levels 155, 245, 315, 390 and 465 (Bulembu Mining Museum).

Asbestos production at the Havelock mine was 1.8 million t between 1939 and 2000 (Gan et al., 2022), making it one of the five largest asbestos mines in the world. According to the last available Manager's Report from February 2000 (Bulembu Mining Museum), "the mine ceased all underground production on January 25, 2000 [and] tailings treatment (alone) began at the beginning of March. […] The underground workshops have been stripped of useable materials and flooded. Water ingress has been far faster than expected. This has been exacerbated by the unusually heavy rains being experienced in the region". According to former manager and worker Phil Wikberg (see also supplementary information SI1) and Darron Raw, "all the tracks on levels 550 and 465 were removed before the levels were flooded. The two vertical shaft skips were not operational when the flooding began. One skip (ore convince) was scrapped at the surface before the headgear was removed, while the main cage for men and material was cut up at the surface" (pers. comm. Phil Wikberg 2023) and "the drainage adit had Furgerson 45 pound steel arch supports which were probably reclaimed to close the portal and prevent access to the old workings at this level – it's anybody's guess what the salvage people removed" (pers. comm. Darron Raw and Phil Wikberg, 2023).

Close to the South African boarder, 1.2 km west-south-west of Bulembu, there is a flooded inclined shaft and an exploration mine in the serpentinite. Outcrops of asbestos are found at both sites. Although detailed documentation of this site could not be found, it is very likely that these are remnants of the Lonrho Limited (UK) asbestos exploration in the 1970ies, mentioned in Dean (1978) and Swaziland Ministry of Commerce Industry and Mines (1970). The mine water in the incline shaft was sampled within this project (sampling location HIS).

No records about the volume of the mined voids, and consequently the volume of the mine pool, could be found. Based on a mass of 25.1 million t of tailings (Gan et al., 2022), a production of 1.8 million t and a rock density of 2.6 kg/t, the mined volume is around 10 million m^3. Using the production of 1.8 million t and a 5.5% rock fibre content (Barton, 1986), 12.6 million m^3 of mined volume can be calculated. Because roughly 80–90% of the mine is flooded, the mine pool comprises 8–11 million m^3 of mining influenced water (MIW), on average very likely 9.5 million m^3 of water. Based on an average flow rate of 3192 L/min, the mine could have been flooded within 5–6 years, giving a first flush period of 15–30 years (average 22 years). This leads to the conclusion, that the first flush is already in the outgoing tail, implying that MIW quality will not further improve in the future.

3. Geological setting

Bulembu is located within the Onverwacht Group of the Barberton Supergroup. Overlying the Onverwacht Group are the Fig Tree and Moodies Groups which all form the eSwatini part of the Barberton Supergroup (Fig. 4a). This Supergroup, which is famously known for its oldest granite-greenstone belt (since 2018 the Barbeton Makhonjwa Mountains UNESCO World Heritage Site; Grobbelaar et al., 2019), ranges from 2700 to 3500 Ma of age (Johnson et al., 2006; UNESCO, 2018). Mafic and ultramafic rocks such as Komatiitic basalt and serpentinite dominate the lower, middle and some upper part of the group, while sedimentary rocks like greywacke/sandstone and metamorphic rocks like pseudochert are visible on the upper most part of the group (Fig. 4b)(Anhaeusser, 1986; Barton, 1986; Ward, 1995). All rocks, including the banded iron formation, banded cherts, talc, and diabase dykes around Bulembu were subjected to extensive metamorphism and deformation. This is even visible in underground workings of the abandoned Havelock mine with metamorphic rocks such as quartzite, granite-gneiss and biotite-mica schists occurring in close contact with chrysotile asbestos host rocks (serpentinite and partly dunite). However, the most visible and dominant rock in the Bulembu area is the deformed serpentinite (Fig. 5a) which is found in the Zwartkoppie Formation (Mendon Fm) of the Geluk Subgroup (Barton, 1986; Johnson et al., 2006) and dunite which can be located mainly underground of the abandoned Havelock asbestos mine (Fig. 5b).

The Barberton greenstone belt hosts a variety of mineralisations such

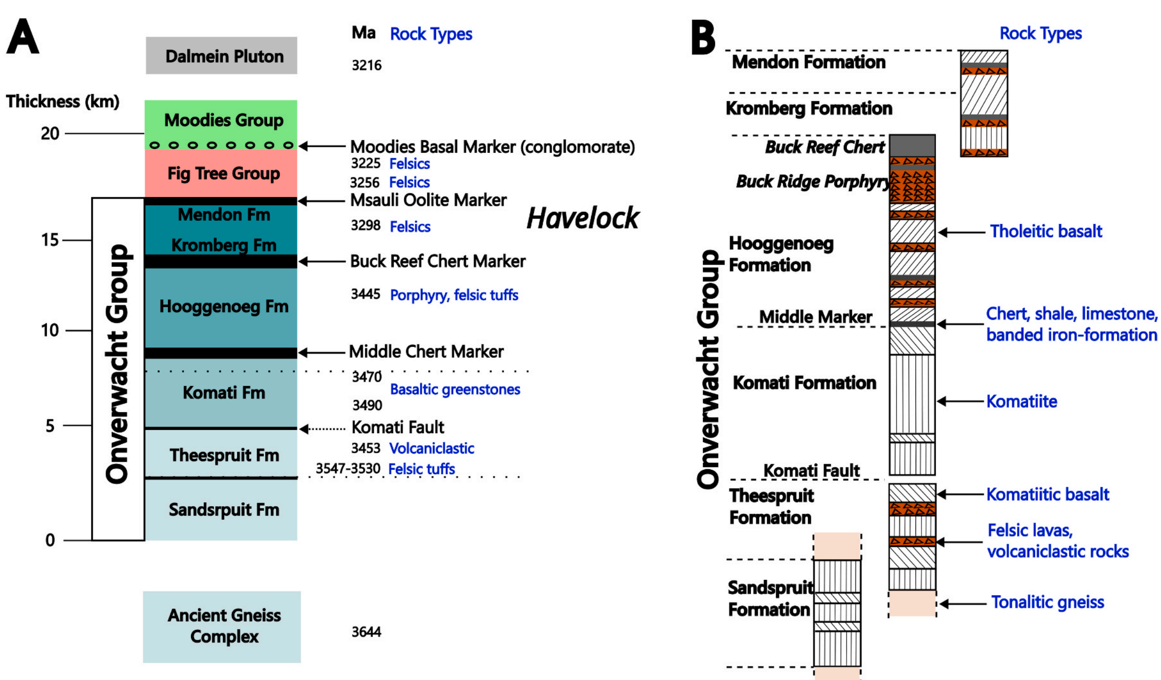

Fig. 4. a) Stratigraphy of the Barberton Supergroup, b) Stratigraphic sections of the Onverwacht Group (modified after Barton, 1986; Ward, 1995).

Fig. 5. Left: Picture of the Serpentinite outcrop in Bulembu (width 15 cm), right: Picture of a dunite outcrop from the Havelock abandoned mine (12E service winze, width 30 cm).

as chrysotile asbestos, gold, talc, or barite (Hall, 1918; Ward, 1995). In the Bulembu–Barberton area, large amounts of cross-fibre chrysotile asbestos from ultramafic rocks of the Onverwacht Group associated with the Mendon Formation (Hofmann et al., 2021) occur and were mined in the Havelock mine, which accounted for roughly 70% of the mined chrysotile asbestos in the greenstone belt and the Msauli mine with 15% (Ward, 1995). The cross-fibre chrysotile asbestos seams and veins occur stockwork like in the deformed serpentinite (Johnson et al., 2006; Wrucke, 1995), and in some places in the altered dunite host rocks (Johnson et al., 2006), with a general E–W to NE–SW strike and at a 45–70° angle. Additionally, the host rocks are characterised by substantial faulting, fracturing, folding and weathering. In most places, host rocks contain quartz and carbonate mineral veins (e.g. calcite) which explains the high mine water pH values of up to 9 and the large concentrations of hydrogen carbonate (further details in section “Results and Discussion”). In the underground workings of the Havelock mine, the outcrops vary in colour from pale green to dark green, with the serpentinite (pale green) mostly dominant on the upper parts of the mine and dunite (dark green) being dominant on the lower parts. Not all the underground outcrops contain chrysotile asbestos of economic value, though the texture is the same as that of the mined chrysotile asbestos.

Barton (1986) identified various minerals, including olivine, orthopyroxene, chromite, brucite, magnesite and carbonates using laboratory analysis. Additionally, quartz, talc, pyrite, calcite, chalcopyrite and gypsum were discovered during this study’s underground investigation. In a recent study, analysing the asbestos tailings by XRD, Gan et al. (2022) found Chrysotile (47%), Lizardite (13%), Magnesite (16%), Talc (5%), Dolomite (5%), Brucite (2%), Chlorite (4%), Quartz (1%), Diopside (4%), Enstatite (0.2%), Forsterite (2%), Hornblende (0.2%), Biotite (0.2%), Pyrite (0.2%) and Magnetite (0.5%; values rounded). Chemical analysis of serpentinite show MgO concentrations between 39 and 44 %, SiO_2 between 37 and 40% and Fe_2O_3 and Al_2O_3 ranging between 1 and 7% (Table 1).

Table 1
Chemical rock and mineral analyses from the Havelock mine. [1]Dark green serpentinite, [2]Light green serpentinite with Chrysotile veins (average ore body rock: dunite), [3]Good quality (19 mm) chrysotile fibre in light green serpentinite (dunite). From van Biljon (1959), cited in Anhaeusser (1976). [4]Chrysotile from cross-vein fibres (Schapira et al., 2023).

Element	Serpentinite[1]	Serpentinite[2]	Chrysotile[3]	Chrysotile[4]
SiO_2	36.91	33.82	39.96	42.08
Al_2O_3	3.52	1.57	0.85	0.59
Fe_2O_3	6.87	3.91	3.67	2.00
FeO	0.14	0.07	0.07	–
MgO	39.07	44.49	40.66	40.83
CaO	0.36	0.10	0.24	0.06
Na_2O	0.15	0.15	0.30	0.07
K_2O	0.12	0.12	0.12	0.01
TiO_2	0.05	0.08	0.08	0.03
P_2O_5	0.08	0.06	0.06	0.01
MnO	0.09	0.05	0.06	0.03
NiO	–	–	–	0.19
CO_2	0.18	0.11	0.13	–
H_2O	13.00	15.52	13.46	12.18
	100.54	100.05	99.66	100.08

4. Hydrology and hydrogeology of the Bulembu area

eSwatini has relatively wet hot summers and cold dry winters, and there is considerable potential for groundwater exploration and surface water utilisation. This is particularly true for the geological setting of the Bulembu area which is dominated by watercourses such as the Tutusi (“Tutuz” in earlier publications, e.g. Hall, 1931) and Nkomazana rivers (e.g. Piteau Associates Engineering Ltd., 1992; UN Department of Technical Cooperation for Development, 1989), which drain into the Komati River Basin (Mlilo et al., 2008). Surface water in the Bulembu area is mainly influenced by the geological setting, farming and post-asbestos mining but is predominantly in pristine conditions (Fig. 6). Investigations conducted show that the surface water in the area is clean with pH values ranging from 7 to 8 (Table 2). The high pH values are influenced by the presence of carbonates such as calcite, dolomite or magnesite, and the total dissolved solids (TDS) are reported to reach even below 30 mg/L in some Highveld streams (UN Department of Technical Cooperation for Development, 1989). Except data in a paper from 1974 (Mazor et al., 1974) and in the Piteau Associates Engineering Ltd. (1992) report, no publications about the stable isotope composition of waters in eSwatini could be located.

Flow rates in the Tutusi river are around 60–85 L/s (rounded to nearest 5 L/s) and in the Nkomazana river twice as much, reaching 150–200 L/s (Table 3). Though only a small number of flow measurements are available, they reflect the seasonal changes, with lower flow rates in the southern hemisphere summer season and higher ones in the winter season. This might indicate that the residence time of the precipitation in the soils and the fractured aquifers is around half a year. Further studies in the Bulembu area are needed to verify these results in more detail.

From the investigations conducted, the Bulembu area has several productive hydrogeological and hydrological units in the Greenstone Belt, weathered greenstone-basalts and fault zones, with the before mentioned average flow rates of 60–85 L/s in the Tutusi and 150–200 L/s in the Nkomazana rivers (Table 3). eSwatini is in an area, where major climatic zones overlap and is consequently influenced by different climatic characteristics, dominated by a sub-tropical climate with relief controlled rainfall (UN Department of Technical Cooperation for Development, 1989). Bulembu lies on the Highveld (Inkangala) and within the Köppen–Geiger zone Cwa (humid subtropical climate), receiving rainfall which might reach monsoon characteristics throughout the year. The Highveld is the coolest and wettest area of eSwatini, receiving an average

Fig. 6. Pristine conditions of the Nkomazana river north-east of Bulembu (left image) and the Tutusi river in Bulembu (right image).

Table 2
On-site parameter results, EC: electrical conductivity; Redox corrected to HSE; –: malfunctioning of the O_2-probe or parameter not determined.

Location	Date	Temp, °C	EC, μS/cm	TDS, mg/L	pH, –	O_2, mg/L	O_2, %	Redox, mV
BWS	2024-02-14	19.9	11	<10	6.46	8.0	102	461
TRB	2022-12-11	20.9	35	34	7.37	7.2	94	413
	2023-05-11	17.3	34	28	7.20	8.6	101	409
	2023-06-24	14.4	38	–	8.30	–	–	437
	2024-02-13	21.1	36	12	7.26	7.7	100	375
TTO	2023-05-13	16.5	60	–	7.67	–	–	451
	2024-02-16	21.1	71	–	8.03	7.5	98	444
TRP	2023-05-10	18.5	64	50	7.73	8.5	100	480
	2024-02-14	19.1	75	32	8.03	8.3	101	480
SWT	2022-12-11	21.1	31	34	6.73	6.9	88	476
	2023-05-10	19.0	30	40	6.71	7.7	94	460
	2024-02-16	21.4	35	16	6.96	7.3	94	458
NKH	2023-05-11	17.6	25	30	7.62	6.3	75	421
	2024-02-14	20.5	27	<10	7.11	8.0	100	383
BWF	2023-05-11	16.4	38	36	7.37	8.0	93	445
	2024-02-14	19.7	44	18	7.40	7.8	98	363
OBW	2023-05-10	19.3	66	60	7.52	8.0	98	392
	2024-02-14	19.6	64	28	7.65	7.9	97	364
BUB	2016-08-25	–	101	73	7.83	–	–	–
	2024-02-14	21.2	83	30	6.58	7.7	104	478
WRP	2022-12-11	25.0	670	428	8.62	4.8	66	360
	2023-05-11	18.0	599	374	8.96	7.4	90	431
	2024-02-13	22.5	806	430	8.63	5.8	76	333
HMD	2022-12-09	21.4	318	238	8.74	5.6	74	441
	2023-05-10	22.7	329	212	8.67	5.9	78	461
	2023-06-24	20.9	363	–	8.60	–	–	439
	2024-02-16	21.6	353	192	8.72	5.3	68	456
10E	2023-05-12	20.7	322	246	8.63	3.1	41	442
	2024-02-13	21.2	345	214	9.10	2.2	28	467
1EA	2023-05-12	19.7	267	–	8.21	–	–	440
	2024-02-13	19.7	303	168	8.52	2.4	30	489
HIS	2023-06-25	19.7	167	80	8.55	–	–	407
	2024-02-13	20.2	167	68	8.71	0.4	5	471

annual rainfall between 840 mm and 1870 mm (1981–2023 data, pers. comm. Dr Owen Buchanan) and covers 29% of the countries area (UN Department of Technical Cooperation for Development, 1989). In Bulembu, the highest rainfall is recorded from September to March (spring and autumn seasons) and maximum rainfall usually in January or February. Lowest rainfalls are from April to August with the minimum rainfall usually in May or June. In spring and autumn, Bulembu receives warm tropical air which results in rain and cold weather, with the Bulembu area receiving rainfall for at least 99–134 days in a year (e.g. Piteau Associates Engineering Ltd., 1992; pers. comm. Dr Owen Buchanan).

Groundwater and surface water temperatures are influenced by air temperatures, thus making the annual air temperature hydrogeologically and hydrologically important. Groundwater and surface water temperatures vary in eSwatini, with the Highveld region temperatures ranging from 16 °C to 23 °C (Piteau Associates Engineering Ltd., 1992) and in the investigated Bulembu area from 14 to 25 °C (underground and surface water temperatures, Table 2) with a temperature high of 36 °C (UN Department of Technical Cooperation for Development, 1989). The same report also concluded that based on a low number of chemical analyses, the water in the Highveld is assumed to meet WHO quality criteria.

Because mining caused the diversion of the Tutusi river from the Mzilanti into the Nkhomazana catchment, the calculation of the mine site's catchment can't be done by using the area of the Tutusi river catchment by itself. Using the average 2020–2022 Bulembu rainfall (1507 mm) and the discharge from the mine (3192 L/min), an area of 1.09 km^2 could be calculated, which coincides with the measured area of 1.1 km^2 for the mine's catchment area. Predominant rocks in this catchment are waste rocks from underground mining, asbestos backfilled into the open pit mine, serpentinites, dunites and rock from the banded iron formation.

Table 3
Flow measurement results in the Bulembu area and the Havelock mine site. EC: electrical conductivity.

Location	Date	Flow rate, L/min	EC, µS/cm	Average Flow rate, L/min
TRB	2023-05-10	4734	37	4294
	2023-06-24	3408	36	
	2024-02-13	4740	36	
TRP	2023-05-09	5172	71	5157
	2024-02-14	5142	75	
NKH	2023-05-11	9090	25	10440
	2024-02-14	11790	27	
WRP	2022-12-11	1	670	1
	2023-05-11	1	599	
	2024-02-13	1.1	806	
HMD	2022-12-09	2893	318	3192
	2023-05-09	3342	363	
	2023-06-25	3174	360	
	2024-02-16	3360	353	
1EA	2023-05-12	235	267	265
	2024-02-13	294	303	
SWT	2022-12-11	50	31	42
	2023-05-10	62	30	
	2024-02-16	14.4	35	
OBW	2024-02-14	14.4	64	14

According to UN and FAO drinking water databases, eSwatini has no specific national guidelines for drinking water quality in place, though the Water Bill 2000 requested their establishment (Government of Swaziland, 2000). Instead, based on the National Water Policy, the National Water Authority "shall promote consistent supply of safe and quality drinking water based on international standards, norms, and best practices" (Government of eSwatini, 2018). Therefore, eSwatini uses the up-to-date WHO drinking water guidelines (World Health Organization (WHO), 2017).

5. The legacy of asbestos mining – asbestos health issues

All types of asbestos are recognised health hazards by OSHA (Occupational Safety and Health Administration) as well as EPA (Environmental Protection Agency), and the fibres associated with health risks are often very small (McCulloch and Tweedale, 2008). These asbestos fibres are the diameter of a human hair, but when inhaled, the tiny fibrils will enter the lungs. Besides the airborne fibres, also waterborne fibres can cause a health hazard (Avataneo et al., 2023; Scott and Hays, 1975). Since the turn from the 19th to the 20th century, it is known that prolonged asbestos exposure and inhalation can cause lung cancer, mesothelioma, diffuse pleural fibrosis, pleural effusions, pleural plaques and in scarring of the lungs called asbestosis which may lead to reduced lung capacity and eventually death (Phillips et al., 2012; Ross, 1999). The type of disease that will develop is usually a function of the fibre length and its diameter (Baron, 2016). In addition, epidemiologists have shown that chrysotile (the most used form of asbestos) also causes the cancer variant mesothelioma in humans (Ross, 1981; Yu et al., 2012) and animals such as guinea-pigs, vervet monkeys, rhesus monkeys and rabbits (Wagner, 1963; Zaidi et al., 1973). Wagner's exceptional research at the South African Pneumoconiosis Research Unit unambiguously showed the link between asbestos and miners' health problems. However, the opposition he faced from the mining industry ultimately forced him to leave South Africa (McCulloch and Miller, 2023).

McDermott et al. (1982) showed in a study from Havelock, that the duration of the exposure is a key determining factor for the deterioration in lung function, which has already been shown by the animal studies of Wagner (1963). In detail, McDermott et al. (1982) noted that surface workers have a lower exposure compared to workers in road sweeping or the grading and milling sections, indicating that the observed changes in parenchymal function are directly related to the type of job the workers conducted. It is unlikely that any of the workers were not exposed, as dry and windy conditions would have blown the asbestos throughout the mine (supplementary information SI1). Furthermore, the study concluded that smoking was not considered relevant for mesothelioma development.

As early as in 1899, Britain factory inspectors noted the dangers of inhaling asbestos, and in 1920 the first medical description of asbestosis was made as fibroses of the lungs, caused by asbestos fibre inhalation. This results in a decreased lung elasticity and consequently shortness of breath (Bartrip, 2000; McCulloch, 2005). Merewether and Price (1930) headed a government inquiry in 1928 and their report established that half of the workers with an exposure time of more than 10 years developed serious asbestosis even after the immediate exposure ceased. Workers' ages on the other hand are of less relevancy than exposure times. Between 1926 and 1930, George Slade conducted research at T&N's New Amianthus mine on the effects of dust inhalation by miners noting that asbestos caused diseases and weakening of the immune system (Slade, 1930). Around the same time, Pim (1932) noticed that future working conditions at the Havelock crushing mills will expose the miners to asbestos resulting in a pulmonary disease which he identified to be asbestosis. Ten years later, measurements showed that the dust concentrations in the mill exceeded 2000 ppcc (part per cubic centimetre) and nearly 66% of the underground samples exceeded the assumed safety level of 300 ppcc (Moerdyk, 1943).

Hilton C. Lewinsohn, who visited Havelock in 1976, reported: "I was in two minds as to whether I should enter the grading mill without the protection of a positive pressure respirator. Going through the mill to the storage shed and then through the shed was frightening. The operative sitting in a glass box and operating the scoop which feeds fibre to the conveyor was covered in fibre. I was astonished to see a man poking at a blocked screw conveyor and creating clouds of dust all about him" (cited in Tweedale, 2001).

With so much information about the dangers of asbestosis, how could T&N ignore all the warnings about asbestosis and allow their workers to continue working in unsafe conditions? The following facts might have helped (partly based on McCulloch, 2005; McCulloch and Miller, 2023; McCulloch and Tweedale, 2008; Thives et al., 2022):

Demand for asbestos was at an all-time high before the Second World War and peaked in the 1970's. T&N threaten to close the mine if they were pressured about the safety for miners which would have come at a huge price tag. Demand for fibre and profits outweighed safety costs for workers. Miners and their families came normally from poor communities that depended on them for employment, and with no trade unions or regulatory bodies in place, worker protection was virtually nonexistent. The extremely bad working condition and low pay wages resulted in a high turnover of workers, so monitoring and recording data of sick workers was difficult, although there were clear indications of health problems. The medical examiners were also not interested in occupational health. T&N's appointed regional manager Roland Starkey gave false information regarding the number of fibres and the company continued to deny that asbestosis exists at Havelock. SA Department of Mines carried out inspections at Havelock, but the system relied on compliance from T&N and had no authority to do anything about dangerous working conditions.

For over 50 years T&N benefitted huge monetary success while exploiting hardworking people that depended on them for a meagre income. Even though the company had all the information about the hazards of working in an asbestos mine, they neglected to inform the workers, did nothing to decrease the dust, prevent inhalation or put in place proper medical care and compensation (Bartrip, 2001; Kazan-Allen, 2003). The legacy left behind is absolutely shameful (e.g. John, 2020). People are dying without money, while the company that should be responsible for their care has long since left the area, despite being well aware of the workers' illnesses (Fig. 7).

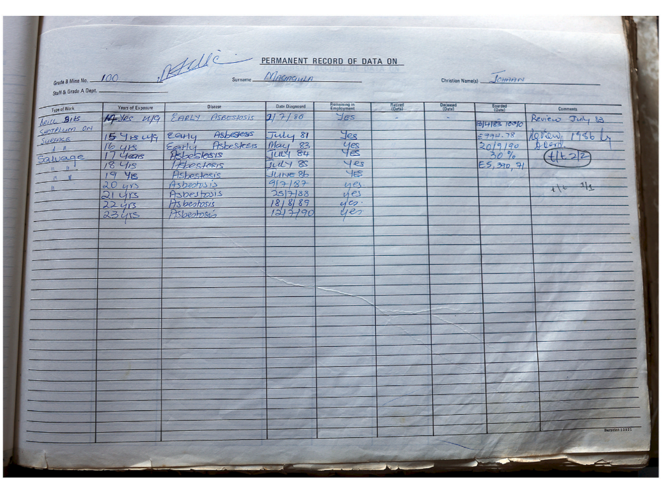

Fig. 7. Sample page from the Havelock miners "Permanent Record of Data" health records proving that miners at the Havelock mine developed asbestosis but were removed from work once diagnosed (held at the Bulembu Mine Museum, miner's family name blurred for data protection).

6. Methods

6.1. Water samples

Twenty-eight water samples from 13 locations (supplementary information SI2) were taken during four sampling campaigns between 2022 and 2024 and chemically analysed for main ions and trace elements as well as stable water isotopes (2023 campaign). In addition to these 13 locations, on-site parameters were determined at an additional two locations, and flow rates were measured at eight locations (Tables 3–5). All sample locations were chosen as such that the background water chemistry in the mining uninfluenced area and the chemistry of water within the mining influenced area could be evaluated. An additional sample from the Bulembu bottled water works (BUL) was included in the interpretation. Three of these sampling locations are mine water samples, of which two were taken underground (10E, 1EA) and one at the mine water discharge (HMD). Access to the mine water table through the main vertical shaft (HVS), which is 107 m below shaft collar, was initially not possible as the accessible part of the shaft was blocked with debris at a depth of 99 m.

Water samples at these 13 locations (BWS, BUB, BWF, TRP, OBW, HMD, SWT, WRP, TRP, NKH, 10E, 1EA, HIS) were taken in 1.5-L PET bottles (unfiltered, main ions) and 50–125 mL HDPE bottles (filtered with 0.45 μm Sartorius PES, trace elements). Trace element samples were acidified with HNO_3 to stabilize the (semi-)metals in the sample. In addition, one sample from the Bulembu Bottled Water works, originating from their borehole, from 2016 was added (sample HLM-2508-BUB). Samples for water isotope studies were sampled in 2 mL opaque glass vials.

6.2. On site parameters

On site parameters (pH, redox potential, EC, LDO O_2-concentration and saturation, temperature) were determined using a HQ40d multimeter (Hach company, Loveland, USA). In addition, the acid and base capacity was analysed by titration using a Hach Digital Titrator (locations TRP and WRP only). Total iron (FerroVer method) and sulfate concentrations (SulfaVer method) were measured with a Hach DR900 Colorimeter (sample locations HMD and WRP) and a Hach DR1900 Spectrophotometer (TNT method, sample location 10E). Oxygen saturation could not be measured on and after 2023-05-12 because of a malfunctioning of the LDO probe. In December 2022 a depth profile was taken in the Havelock vertical shaft using a 500 m Ott KL010 TCM contact gauge. Yet, the probe got stuck at a depth of 125–130 m below shaft collar (≈20 m below the water surface).

At sampling locations TRB and HMD, van Essen CTD divers were installed between 2023-05-09 and 2023-06-24 (46 days). They measured the water temperature, EC and the water pressure above the sensor at 5 min sampling intervals.

Along the course of the Tutusi diversion tunnel, on-site parameters were measured every 40 m to identify the reason for the electrical conductivity increase between the inflow (TRB) and the outflow (TTO) of the tunnel.

In the SW compartment a shaft logging with a Sea & Sun CTD48M multiparameter probe (Sea & Sun Technology, Trappenkamp, Germany) was conducted down to a water depth of 183.2 m. That probe measures electrical conductivity, temperature, pH and the pressure up to a water depth of 1000 m.

6.3. Flow measurements

Three methods were used to determine the flow rates at the different sampling locations (detailed descriptions can be found in Wolkersdorfer, 2008). At sampling locations SWT, OBW and WRP (locations are provided in Fig. 2), the flow rates were measured with the volumetric method ("bucket-and-stopwatch"). Furthermore, the salt dilution method (sudden-injection gulp method) was used at sampling locations TRB, HMD, NKH and TRP (TQ Tracer Mobile Discharge Measurement System, Sommer Messtechnik, Koblach, Austria). For this method, 1–1.5 kg of NaCl were dissolved in a bucket with approximately 20 L of stream water. This solution was gulp injected upstream the measurement location at a distance of approximately 25–50 times the width of the stream to allow for an adequate mixing length. At the measurement location, two electrical (EC) conductivity probes were placed in the main flow at distances of one third of the stream width from the stream banks. Prior to their installation, the conversion factor from EC to the NaCl concentration was determined by a multiple point calibration. The breakthrough curve was recorded using the TQ Tracer system and the TQ Commander software (Sommer Messtechnik, Koblach, Austria), which also calculated the flow rates. Finally, at sampling location 1EA, the area-velocity method using a floating device was used.

6.4. Tracer tests

Two kilograms of **sodium chloride** (CAS 7647-14-5) dissolved in 20 L of local tab water were injected into the Havelock vertical shaft (HVS) in December 2022. For tracer detection by electrical conductivity, a van Essen CTD Diver was installed at the discharge adit (HMD) and a sampling rate of 20 min was programmed. The water level was at ≈ 107 m below

Table 4
Trace elements concentrations (filtered) in mg/L of the Bulembu water samples. For comparison, WHO drinking water guidelines 2017 and USEPA MCL (EPA 816-F-09-004) are listed in the last rows. Trace elements below the detection limits are not listed here.

Location	Date	Sr	Ba	PO_4	B	Br	As	Cr	Fe	Mn
BWS	2024-02-14	0.002	0.001	0.31	<0.025	<0.1	<0.001	0.001	0.039	<0.025
TRB	2022-12-11	<0.010	<0.010	0.05	<0.025	<0.1	<0.010	<0.010	<0.025	<0.025
	2023-05-11	<0.010	<0.010	0.04	<0.025	<0.1	<0.01	<0.010	<0.025	<0.025
	2024-02-13	0.004	0.002	<0.31	<0.025	<0.1	<0.001	0.002	<0.025	<0.025
TRP	2023-05-10	<0.010	<0.010	0.03	<0.025	<0.1	<0.01	<0.010	<0.025	<0.025
	2024-02-14	0.007	0.004	<0.31	<0.025	<0.1	<0.001	0.003	<0.025	<0.025
SWT	2022-12-11	<0.010	<0.010	0.10	<0.025	<0.1	<0.010	<0.010	0.030	<0.025
	2023-05-10	<0.010	<0.010	0.05	<0.025	<0.1	<0.01	<0.010	<0.025	<0.025
	2024-02-16	0.002	0.005	<0.31	<0.025	<0.1	<0.001	<0.001	<0.025	<0.025
NKH	2023-05-11	<0.010	<0.010	0.03	<0.025	0.1	<0.01	<0.010	0.028	<0.025
	2024-02-14	0.004	0.002	<0.31	<0.025	<0.1	<0.001	0.001	0.053	<0.025
BWF	2023-05-11	<0.010	<0.010	0.06	<0.025	<0.1	<0.00	<0.010	0.030	<0.025
	2024-02-14	0.005	0.003	<0.31	<0.025	<0.1	<0.001	0.001	<0.025	<0.025
OBW	2023-05-10	<0.010	<0.010	0.04	<0.025	<0.1	<0.01	<0.010	<0.025	<0.025
	2024-02-14	0.003	0.003	0.31	<0.025	<0.1	<0.001	0.006	<0.025	<0.025
BUB	2016-08-25	–	–	–	–	–	–	–	0.031	0.008
	2024-02-14	0.004	0.002	0.31	<0.025	<0.1	<0.001	0.003	<0.025	<0.025
WRP	2022-12-11	0.013	0.010	0.13	<0.025	1.2	<0.010	*0.096*	0.050	0.03
	2023-05-11	0.016	0.010	0.10	<0.025	0.6	<0.01	*0.136*	<0.025	<0.025
	2024-02-13	0.017	0.013	0.31	<0.025	<0.1	<0.001	*0.092*	0.034	0.025
HMD	2022-12-09	0.016	0.011	0.10	1.410	0.3	*0.056*	<0.010	<0.025	<0.025
	2023-05-10	0.021	0.014	0.04	<0.025	<0.1	*0.072*	<0.010	<0.025	0.025
	2024-02-16	0.017	0.012	0.31	1.43	<0.1	*0.058*	0.004	<0.025	<0.025
10E	2023-05-12	0.016	0.014	0.06	<0.025	0.1	*0.083*	<0.010	<0.025	<0.025
	2024-02-13	0.014	0.013	0.31	1.38	<0.1	*0.064*	0.008	<0.025	<0.025
1EA	2024-02-13	0.014	0.004	0.31	0.032	<0.1	0.005	0.018	<0.025	<0.025
HIS	2023-06-25	<0.010	<0.010	<0.1	0.140	0.2	<0.010	<0.010	0.033	<0.025
	2024-02-13	0.008	0.002	0.31	0.165	<0.1	0.001	<0.001	<0.025	<0.025
WHO	2017 A3.3	–	1.3	–	2.4	–	0.01	0.05	–	–
USEPA MCL	2009	–	2	–	–	–	0.010	0.1	–	–

Table 5
Main ion concentrations in mg/L of the Bulembu water samples. %err: PHREEQC percent error (concentrations below the detection limit were set to half the detection limit in PHREEQC).

Location	Date	Ca^{2+}	K^{+}	Na^{+}	Mg^{2+}	NH_4^{+}	SO_4^{2-}	Cl^{-}	NO_3	HCO_3	SiO_2	%err
BWS	2024-02-14	<1	<0.5	<1	<1	<0.13	<2	2	<0.44	<5	6.2	−17.64
TRB	2022-12-11	3	<0.5	1	3	<0.1	<2	3	<0.1	24	11.6	−5.99
	2023-05-11	2	<0.5	1	2	0.13	<2	2	0.89	24	8.3	−24.93
	2024-02-13	2	<0.5	1	2	<0.13	<2	2	<0.44	15	7.9	−4.01
TRP	2023-05-10	4	<0.5	1	5	0.13	<2	3	2.21	29	9.2	−5.21
	2024-02-14	4	<0.5	1	6	<0.13	2	3	0.44	39	8.6	−3.63
SWT	2022-12-11	2	0.6	1	2	<0.1	<2	3	<0.1	20	13.3	−14.95
	2023-05-10	2	0.5	1	2	0.13	<2	2	0.44	10	10.1	8.57
	2024-02-16	2	<0.5	1	2	<0.13	<2	2	<0.44	15	10.3	−4.01
NKH	2023-05-11	2	<0.5	1	1	0.13	<2	2	1.33	20	8.1	−35.29
	2024-02-14	1	<0.5	1	1	0.13	<2	2	<0.44	10	7.9	−15.70
BWF	2023-05-11	3	<0.5	1	2	0.13	<2	2	0.89	20	8.3	−11.75
	2024-02-14	3	<0.5	1	2	<0.13	<2	2	0.89	20	8.8	−12.60
OBW	2023-05-10	2	<0.5	1	7	0.26	<2	6	3.54	29	10.5	−10.77
	2024-02-14	2	<0.5	2	6	<0.13	<2	4	2.21	34	10.7	−10.75
BUB	2016-08-25	6.59	0.26	8.30	3.56	0.18	5.93	9.05	0.93	41	–	−1.39
	2024-02-14	8	<0.5	1	4	<0.13	<2	3	0.44	44	9.2	−5.09
WRP	2022-12-11	4	4.3	4	116	<0.1	<2	6	0.5	503	4.3	9.22
	2023-05-11	3	3.8	5	91	0.13	3.0	5	5.31	411	2.4	4.63
	2024-02-13	4	2.6	3	115	<0.13	<2	5	1.33	567	3.2	1.75
HMD	2022-12-09	10	11.5	6	33	<0.1	35	15	1.0	142	9.8	3.11
	2023-05-10	10	10.4	6	32	0.26	31	13	5.31	156	7.1	−3.84
	2024-02-16	10	11.2	6	32	<0.13	36	13	3.54	136	7.3	1.13
10E	2023-05-12	11	9.5	6	32	0.13	30	12	5.31	150	7.7	−1.58
	2024-02-13	10	10	6	32	<0.13	33	12	6.20	139	7.9	−1.50
1EA	2024-02-13	17	<0.5	3	29	<0.13	7	4	1.77	190	16.7	−2.00
HIS	2023-06-25	6	<0.5	1	19	0.20	<2	2	0.1	109	4.5	1.34
	2024-02-13	5	<0.5	1	18	<0.13	2	2	<0.44	105	4.3	−1.65

shaft collar, just below the mine's level 3.

Sodium fluorescein (uranine, CAS 518-47-8) was injected at a mass of 503.55 g at the Havelock vertical shaft (HVS) in May 2023. To detect the tracer breakthrough curves, a GGUN-FL surface fluorometer (Albillia SARL – Pierre Schnegg, Switzerland) was installed at location HMD with a logging interval of initially 1 min, later 5 min.

To investigate also the connection from the underground section of the mine with the point of discharge, an additional tracer test was started in February 2024. At location 10E, 1000 g of **Eosin Y** (CAS 15086-94-9) and at location HVS, 1000 g of **sodium fluorescein** (uranine) were injected on 2024-02-13 (17:06) and 2024-02-12 (17:16), respectively. To detect the tracer breakthrough curves, a GGUN-FL surface fluorometer (Albillia SARL – Pierre Schnegg, Switzerland) was installed at location HMD with a logging interval of initially 1 min, later 5 min. Simultaneously, a TRAQUA Stream fluorescent tracer probe (TRAQUA, Namur, Belgium) measured the tracer concentrations at a 15 min interval during the February 2024 test.

Tracer test results were evaluated with a self-programmed MS Excel spreadsheet. Between the sampling location HMD and the injection location HVS, the horizontal distance was 1.1 km, and the tracer is expected to have flown 1.4 km underground. A similar distance of 1.3–1.6 km is expected for the flow distance between 10E and HMD. Tracer background concentration of the first test was 0.78 μg/L, but the reason for this background concentration could not be determined.

On 2024-02-15, a TRAQUA Stream fluorescent tracer probe was lowered into the main vertical shaft (HVS) to measure the uranine tracer concentration down to a water depth of 228 m (335 m below shaft collar) with a spatial resolution of 6.5 m.

6.5. Camera logs

To ascertain if a multimeter probe can be lowered into the vertical shaft, four borehole camera logs were conducted by Boegman Groundwater Specialist (East Lynne, South Africa). The condition of the shaft's compartments below the four boreholes drilled into the shaft's concrete sealing was inspected and any shaft blockages and the depth thereof recorded.

6.6. Chemical laboratory analysis

All samples were analysed at Waterlab (Pretoria, South Africa) SANS accredited lab with a discrete analyser for Cl, SO_4, N and PO_4, titration for alkalinity and ICP-MS for trace and main elements. TDS was determined gravimetrically after drying at 180 °C. Isotope samples were analysed at TU Dresden (Germany) with a mass spectrometer. Sample HLM-2508-BUB (data provided by Bulembu ministries) was analysed by REID-LINE Scientific Services CC (Table View) in non-reported, non-SANS accredited labs.

6.7. Microscopy

Two water samples from the mine discharge (HMD) were investigated microscopically for the occurrence of asbestos fibres. 1500 mL of the water were filtered through a 0.45 cellulose acetate membrane filter (Sartorius, Göttingen, Germany) and mounted to microscopy glass plates. A Zeiss AxioZoom V16 with an AxioCam 712 and transmitted light was used to examine the samples and count the asbestos fibres.

6.8. BART tests

The Biological Activity Reaction Tests (BART™) are microbial tests in vials that allow the detection of unwanted bacteria in water (Cullimore, 1999). They are available for a large range of bacteria commonly found in water. Two different BART investigations were conducted on 15 mL samples from locations HMD, SWT, OBW, BWF, TRP and WRP. These microbial tests determine slime forming (SLYM-test) and sulfate reducing bacteria (SRB-test). Vials were checked daily for any visual changes within them.

6.9. Chemical thermodynamic modelling

Twenty-eight chemical water samples were used for chemical thermodynamic modelling with PHREEQC 3.7.3.15968 (Parkhurst and Appelo, 2013) and the wateq4f database to include the As species.

6.10. Statistics and visualisation

All data were analysed with IBM SPSS 29.0.1.0 using Pearson's correlation, principal component analysis, cluster analysis and random forest. Ion balances were calculated with PHREEQC using the wateq4f database. Visualisation of data was conducted with Geochemists Workbench 17.0.1 and Sigmaplot 15.1.1.26.

7. Results and interpretaton

7.1. Introduction

All results are presented in the tables and graphs of this paper. Additional data is provided in the electronic appendices. Based on these results from various investigation techniques and sampling campaigns, this section discusses them in context, instead of separating the presentation of results and their discussion. Following this section will be the conclusions that result from this.

7.2. PHREEQC and ion balance

PHREEQC percentage errors of the 28 water samples range between −25% and +9%. The high errors predominantly occur with the low mineralised surface water samples (low electrical conductivity), where small concentration variations due to rounding can result in high errors. A random forest analysis revealed that specifically the HCO_3, Mg and Ca concentrations influence the error as they show the highest decrease in node impurity. Therefore, these samples will not be excluded from statistical analysis or results' interpretation.

7.3. On-site parameters and data loggers

On-site parameters show a clear distinction between MIW and uninfluenced water (Table 2). While MIW has higher EC values between 167 and 670 μS/cm, uninfluenced waters range from very low 25 to 66 μS/cm, characteristic for silicate rich rocks, such as serpentinites (Fig. 8) and indicative of low residence times. These values are even lower than the averages for surface water reported by Langmuir (1997). The same is true for the TDS, with the MIW showing substantially higher values (212–428 mg/L) compared to the surface water samples (28–60 mg/L). Sample HIS from the flooded incline shaft has a TDS of 80 mg/L, displaying a transition stage from surface/groundwater to MIW. Temperatures for all waters range between 14 and 25 °C and are identical to earlier findings. pH-values are relatively high, between 7.2 and 9.0, which is due to a lack of acid producing phases on one side and the weathering of the Ca-und Mg-rich rocks together with atmospheric and soil CO_2 to hydrogen carbonate on the other side. MIW samples have high pH values because of the carbonates found in the mine voids. Surface waters are characterised by high oxygen saturation (75–101%), resulting from well mixed, turbulent flow conditions, while MIW has lower oxygen saturations between 41% and 90%, as oxygen is consumed by microbial processes underground and weathering processes in the waste rock pile. This is partly reflected by the redox potential, which, on average, are lower in the MIW (428 mV) compared to surface water (438 mV), though the difference is statistically not significant.

In addition to the individual on-site parameter measurements, van Essen data loggers recorded temperature and EC a locations TRB and HMD. While TRB showed clearly diurnal temperature and EC fluctuations ranging between 12 and 18 °C and 37 to 41 μS/cm, respectively, these parameters showed characteristic underground low pass filtering for HMD. There, temperature ranged around 21 °C with small fluctuations of 0.01–0.02 K and EC values ranged between 260 and 320 μS/cm. This low pass filtering of the mine pool water results from mixing in the large mine pool (9.5×10^6 m³) and water rock interaction which buffers the temperature around the mean annual temperature at Bulembu.

On-site parameters for the Tutusi river upstream (TRB) and

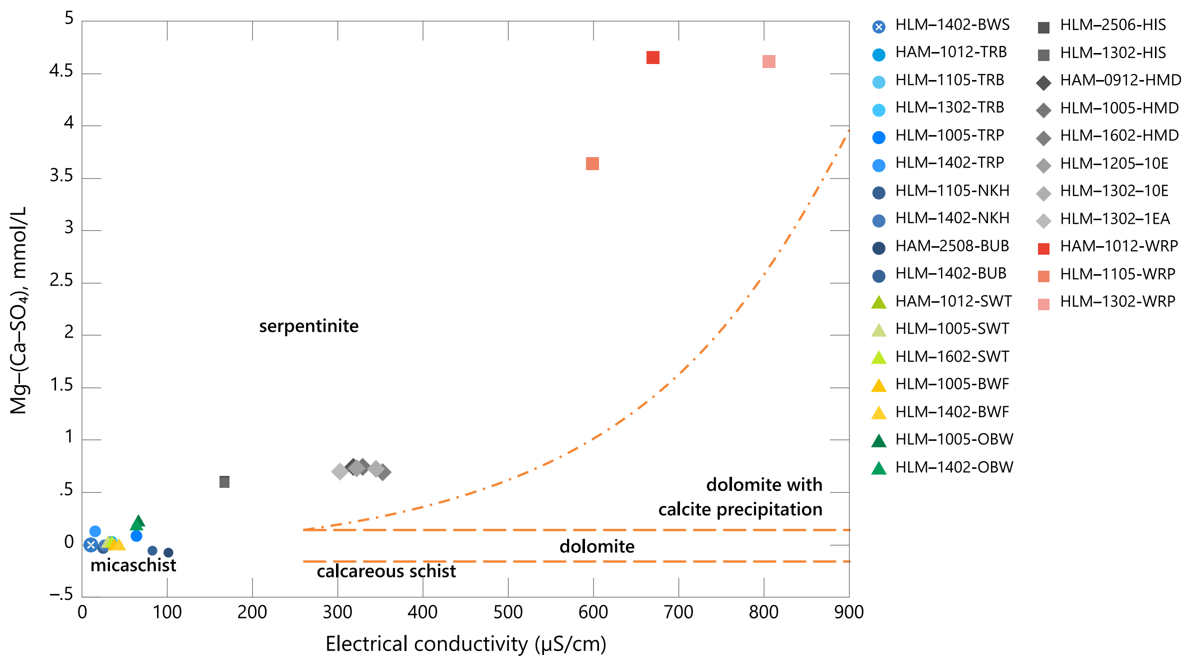

Fig. 8. Scatter plot of electrical conductivity vs. concentration difference of Mg^{2+} and Ca^{2+} (except gypsum Ca^{2+}) of the water samples taken around Bulembu. Diagram type based on Appelo et al. (1983).

downstream (TRP) the diversion tunnel showed an increase in electrical conductivity and pH from 36 to 60 µS/cm and pH 7.13 to 7.88, respectively. Because there was a substantial change in values between the tunnel outflow (TTO) and the downstream sampling location, the reason for that change was expected to occur within the tunnel with the hypothesis of an inflow through the tunnel ceiling. In fact, the electrical conductivity increases during the course of the tunnel, very likely from the inflow of higher mineralised water through the tunnel walls and ceiling. pH first increased, then decreased and the redox potential increased by 120 mV. These results show that here is not an individual inflow responsible for the parameter changes, but very likely the concrete lining of the tunnel.

7.4. Main ions

All the main ions in the surface water samples show very low concentrations (Table 5), explaining the low EC and TDS values. Ca, K, Na, Mg, NH_4, SO_4, Cl and NO_3, all are below 7 mg. This results from the low contact times of the waters with the local rocks and their low solubility in the given meteorological conditions. Only hydrogen carbonate and silica have slightly higher concentrations of 10–29 mg/L and 8–13 mg/L, respectively, showing that the crystalline mafic rocks contain small amounts of carbonate minerals (primary and from weathering), but predominantly soluble silica compounds from mineral alteration and from easier soluble silica minerals in the soils (Langmuir, 1997). de Villiers and de Wit (2007), who studied river water in eSwatini, found substantially higher main ion concentrations in Swaziland Supergroup dominated rivers (TDS 84–819 mg/L), possibly because their river sampling locations were much further away from the spring areas compared to the Bulembu samples.

Nitrate, ammonia and phosphate can be indicative of either agricultural influence, sewage water or explosives from mining. Yet, especially at sampling location OBW (Jamesville Waterfall), which was chosen to get background concentrations, these cannot be explained in such a way. Phosphorous was identified in very low concentrations around the detection limit by Gan et al. (2022) in samples from the Havelock asbestos tailings. It could also originate from the banded iron formation (Hall, 1930) or just in general from the igneous rocks in the Havelock mine (Hem, 1985). All the MIW shows higher concentrations of all parameters except SiO_2. Reason for that is that the SiO_2 coming from the soil has long been either leached or is not a steady source for the MIW. What stands out from the chemical analysis are Mg and HCO_3. Because the molar ratio of Ca and Mg are not 1:1, dolomite dissolution is not the reason for these concentrations (Fig. 8). However, reasons are the weathering of rock forming minerals with atmospheric and biological CO_2 and the dissolution of aragonite/calcite that is abundant underground from both, concrete and rock weathering. Very similar conditions compared to those of Bulembu are described by Appelo et al. (1983) from the Southern Tyrolean Ahrntal (Italy). There, serpentinite spring water showed a pH of 8.47 and EC of 152 µS/cm as well as Mg, Ca and HCO_3 concentrations in the range of the average Bulembu concentrations. Their EC/(Ca–Mg)-Diagram was therefore also used to plot Bulembu water samples (Fig. 8), which plot according to their characteristics as surface water, MIW and waste rock pile water.

7.5. Trace elements

Most analysed trace elements are below the detection limits, specifically in the surface water samples. Only nine elements and PO_4 show at least one sample with concentrations above the detection limits. Except for the MIW samples at locations WRP, HMD and 10E, none of the water samples in the Bulembu area exceeds the limits in the WHO drinking water guidelines (World Health Organization (WHO), 2017). At the waste rock pile seepage (WRP), the total Cr concentrations range between 0.096 and 0.136 mg/L at a flow rate of 1 L/min. This is also the location with the highest Mg, hydrogencarbonate and TDS concentrations (91–116 mg/L, 411–503 mg/L, 374–428 mg/L, respectively) resulting from the exposure of the serpentinite waste rock to the atmosphere and its subsequent weathering (Tables 2–5). Elevated Cr concentrations have also been recorded around naturally occurring asbestos deposits in Italy and were attributed to the rock matrix (Avataneo et al., 2021). Because the Havelock serpentinite contains chromite ($FeCr_2O_4$) and up to 0.57% nominal Cr_2O_3 (Barton, 1986), the source of the Cr can be traced to this mineral. Arsenic, compared to the WHO drinking water guidelines, shows elevated concentrations of 0.056–0.083 mg/L in the Havelock mine pool samples (10E and HMD). A source of the arsenic might be arsenopyrite, which is abundant in Onverwacht Group rocks of the She gold mine area 17 km south-west of Bulembu (Cairncross, 2022) and in the gold occurrences around Piggs Peak and Barberton in general (Hall, 1918; Ward, 1995). No visual arsenopyrite could be identified on the waste rock piles or underground.

As neither the MIW nor the waste rock pile seepage is used as drinking water, mitigation of the slightly elevated Cr or As concentrations is not necessary, as the costs would be disproportionate to the results. In the case of the waste rock pile seepage, the load is low, and at the downstream Tutusi sampling location TRP, the Cr concentration is already below the WHO limit. Should remediation be deemed necessary, it would be necessary to apply an impermeable cover to the entire waste rock pile. It is possible that arsenic concentrations discharging from the adit could be lowered with the installation of a passive mine water treatment system. However, given that surface water is not used for human consumption and that intense rainfall sometimes causes flooding of the rivulet, it is questionable whether this would be a viable solution.

7.6. Piper plot

With the exception of the waste rock pile samples, all the samples plot in the earth alkaline predominantly hydrogen carbonate field (according to Furtak and Langguth, 1967) of the Piper-diagram (Piper, 1944, 1953). This is similar to the findings of Sacchi et al. (2021), who investigated the trace element distribution in the vicinity of a North Italian serpentinite hosted asbestos mine. There is no clear distinction between the Havelock mine pool samples and the Bulembu surface water samples (other than in the EC/(Ca–Mg)-Diagram, Fig. 8), indicating that the differences in the chemical composition of the main ions of these two groups seem to be predominantly related to the contact time of the water with the rocks (Fig. 9). The raw material mineralisation seems not to be reflected by the ratios of the main ions, except Mg, which could also be attributed to the fact of the very low cation concentrations in the surface water samples.

7.7. Statistical analysis and cluster analysis

Principal component analysis (PCA) with 28 samples revealed that three components are responsible for 79% of the samples' variability (Fig. 10). Component 1 (50% of the variability) represents the rock matrix, component 2 (18% of the variability) the mining influences and component 3 (10% of the variability) could be attributed to explosives, still existing in the waste rock and underground. These PCA results show that the water chemistry is predominantly controlled by the rock matrix and that the variability in the area's rock assemblage is not reflected by the PCA results.

Pearson correlation analysis with the parameters available in all samples showed that TDS, EC, pH and the main ions are positively correlated with each other. The highest, and statistically significant correlations exist with Mg, HCO_3 and the EC, all of them with $r^2 > 0.95$ and $p \ll 0.05$.

A cluster analysis was performed on the 10 variables of the first component and a loading greater than +0.5. This cluster analysis confirms what could already be seen from the species plot, that there are three main clusters with one sample (HIS) offset from the others. Based on the cluster analysis it is clear that sample HIS is statistically closer to the surface water samples than to the MIW samples, as can also be seen in the EC/(Ca–Mg)-diagram (Fig. 8). These cluster analysis results clearly show that there are three statistically distinct groups of Bulembu water samples. The first group are the surface water samples, the second group are the mine pool samples and the third group is the water percolating through the Bulembu waste rock pile (Fig. 11). Thought the surface water samples were taken from water courses originating in slightly different lithologies, their chemical characteristics are similar. This means that the differences in the lithologies are not large enough to be reflected by the waters' total chemical composition and the statistical results.

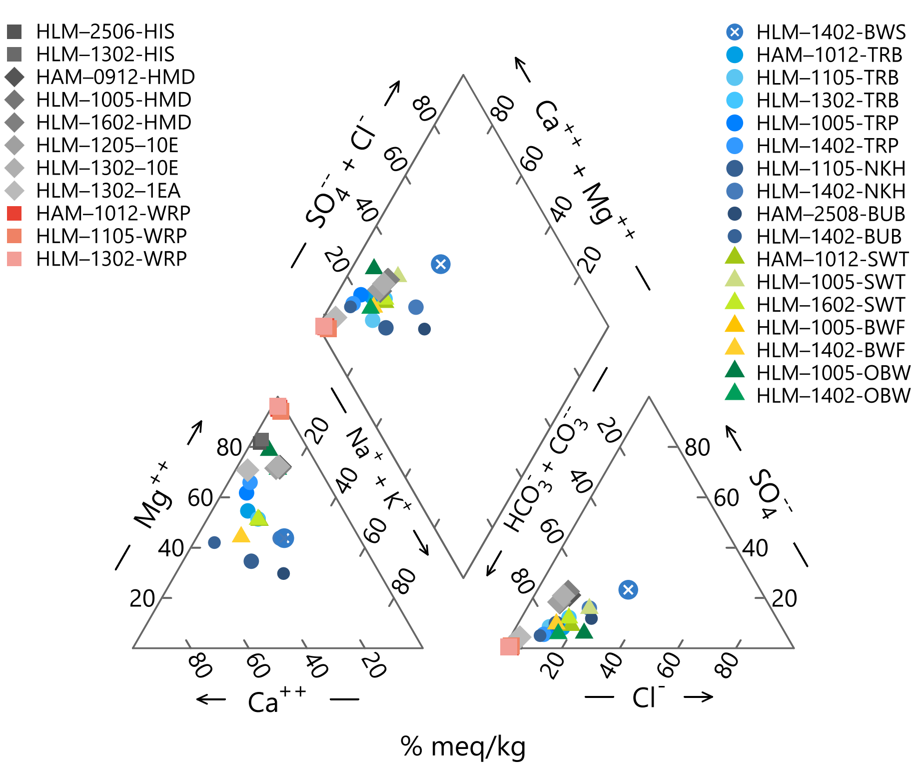

Fig. 9. Piper Diagram of the Bulembu and Havelock surface and MIW samples. Symbols on the left represent mining related sampling points; symbols on the right to surface water samples.

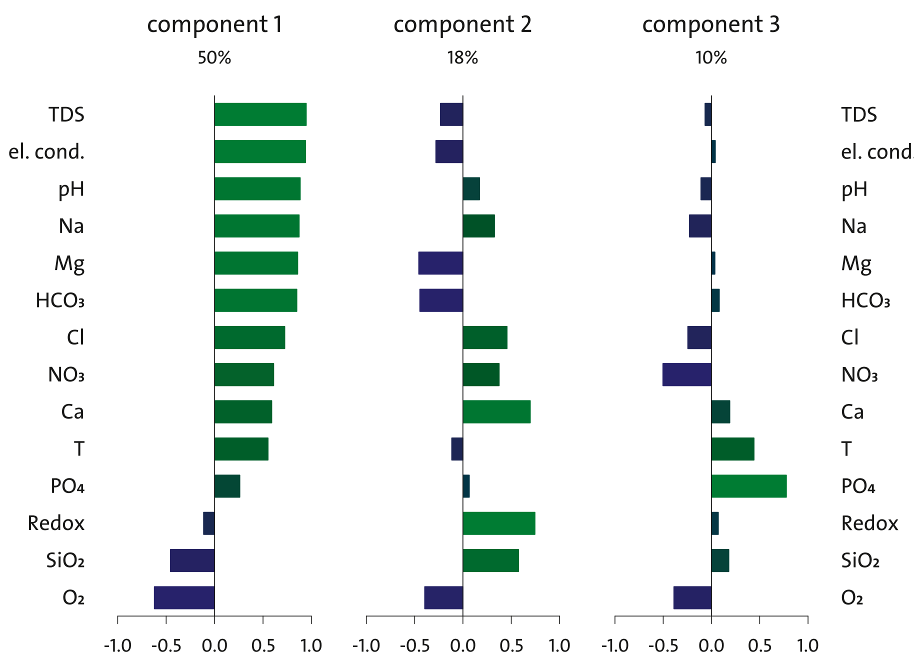

Fig. 10. Principal Component Analysis of the Bulembu surface and MIW samples (excluding sample HAL-2508-BUB; n = 26, cumulative variance: 78.7%).

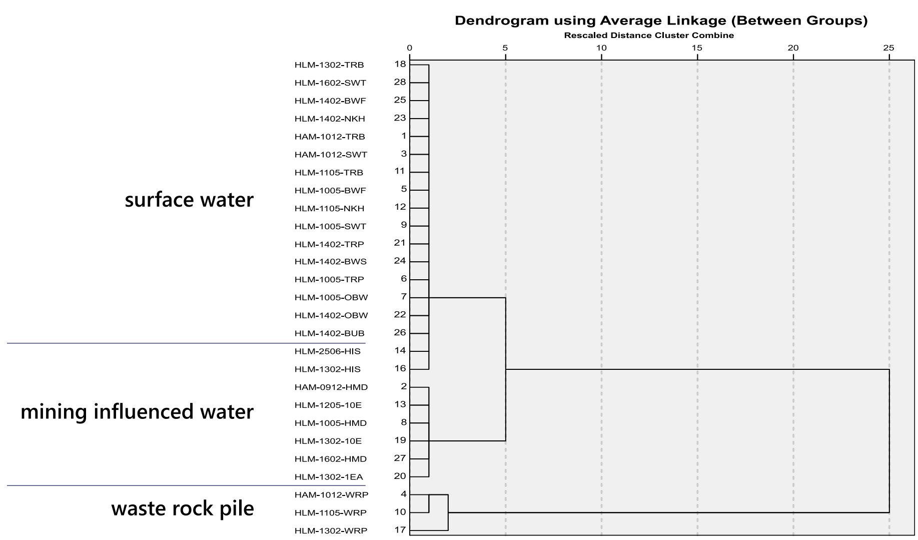

Fig. 11. Dendrogram of the Bulembu and Havelock surface and MIW samples (all parameters with a loading of >0.5 in the first cluster of the PCA were used to calculate the dendrogram).

7.8. PHREEQC results

To interpret the water chemistry, all samples were modelled in the chemical thermodynamic code PHREEQC with the wateq4f database. PHREEQC percentage errors of the 28 water samples range between −25% and +9%. The high errors predominantly occur with the low mineralised surface water samples, where small concentration variations due to rounding can result in high errors. A correlation analysis revealed that it is specifically the Ca concentration that seems to influence the error. Therefore, these samples will not be excluded from statistical analysis or results' interpretation.

To visualise the results, specifically the species contribution to the water chemistry, the molar concentrations were plotted (Fig. 12). This allows both a quick identification of the chemical composition of the water and a comparison between different samples. As can be seen, the 28 samples resemble 3 to 4 groups. All of them are dominated by Mg hydrogencarbonate, also obvious from the Piper-diagram (Fig. 9). The differences between the groups are partly due to the concentration of the species, but also to the K and sulfate concentrations. Sulfate in the mine pool samples comes from (di-)sulfide weathering, specifically pyrite, which could be seen in underground outcrops. Potassium, as the rock analyses show, is underrepresented in the rocks, but very likely comes from micas, such as the biotite identified in the asbestos tailings.

Sample HIS is chemically between the mine pool samples and the surface water samples. It is from a small incline shaft south-west of Bulembu and because of its longer residence time in the flooded shaft, the mineralisation increased. As this abandoned mine was not further explored because of lack of raw material it could be the reason for this sample not showing sulfate concentrations.

Controlling phases are phases (which are minerals *senso lato*) with faster dissolution or precipitation kinetics compared to other phases in the system, and they can be identified by saturation indices (SI) around

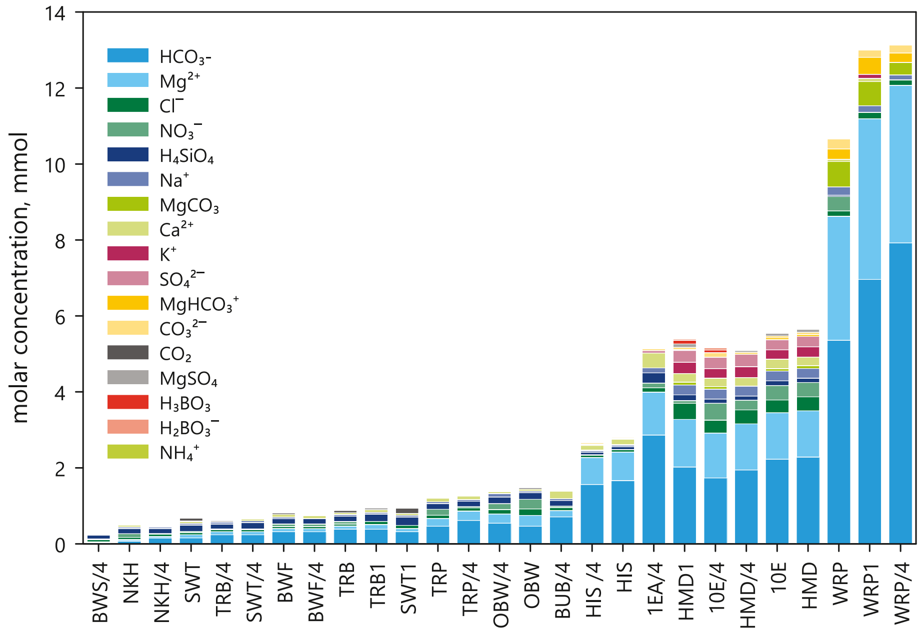

Fig. 12. Molar concentrations of species in Bulembu and Havelock surface and MIW samples (98% of all PHREEQC calculated species considered).

Table 6
Stable isotope composition of the Bulembu and Havelock water samples. unc.: uncertainty.

Location	Date	Lab. №	$\delta^{18}O$, ‰	unc., ‰	$\delta^{2}H$, ‰	unc., ‰
TRB	2023-05-10	W-2023-156	−4.2	0.2	−16.8	1.3
TRP	2023-05-11	W-2023-161	−4.2	0.2	−15.8	1.2
SWT	2023-05-11	W-2023-153	−4.2	0.2	−17.6	1.2
NKH	2023-05-11	W-2023-155	−4.0	0.2	−16.1	1.3
BWF	2023-05-11	W-2023-154	−4.2	0.2	−16.9	1.1
OBW	2023-05-11	W-2023-158	−4.1	0.2	−15.8	1.1
WRP	2023-05-11	W-2023-160	−3.8	0.2	−13.4	1.3
HMD	2023-05-10	W-2023-159	−4.1	0.2	−14.6	1.1
10E	2023-05-12	W-2023-157	−4.1	0.2	−15.9	1.1

0. They, therefore, dominate the final water chemistry of an aqueous solution and contribute substantially to the chemical composition of the solution. Depending on the authors, controlling phases are those with an SI of ± 0.5 or ± 1. In this publication, controlling phases will be considered those which have an SI of ± 1.

Most phases that PHREEQC calculated are undersaturated in relation to the 28 water samples, and therefore only a small number of phases can be discussed as controlling phases. Based on the PHREEQC results, SiO_2 in all the water samples, as expected, is controlled by Quartz, Chalcedony and Cristobalite, less by Silicagel. PO_4 in the surface water samples are controlled by $MnHPO_4$, but this is only a nominal phase, as phosphate might originate from weathered apatite phases not reflected by PHREEQC. In the mine pool, the SI of $MnHPO_4$ is quite low, indicating that it is undersaturated in relation to the mine pool water. Manganite is a manganese oxide-hydroxide, Rhodochrosite a manganese carbonate and Nsutite a manganese oxide, which control the Mn concentrations in the MIW, but because the concentrations are around or below the detection limit, the SI for the three is not clear enough for interpretation. Aragonite and Calcite are controlling the Ca concentrations in the MIW, which can be seen by the SI of ± 0.4. These minerals can be identified by the abundance of stalactites in the mine workings, and the concrete used therein. None of the surface water samples shows a Ca control by these two phases. Diopside ($MgCaSi_2O_6$) and Dolomite have been described for Havelock, and they control the Mg concentration in the mine pool samples and Dolomite also the pH value. Because of the low concentrations of most water constituents, no other controlling phases are relevant for the waters' composition.

Sampling sites HMD, WRP and 10E exhibited saturation indices between 9 and 12, indicating that the water is oversaturated in relation to the two phases in the WATEQ4F database (chrysotile, tremolite). However, kinetic factors prevent their precipitation in all three sampling sites that are related to the mining operation. HMD is the outflow of the mine pool, WRP is the waste rock pile, and 10E is an underground water sample. While these three sampling sites provide insight into the presence of asbestos in the rock, the asbestos itself does not contribute to the overall chemistry of the water, as previously described.

7.9. Stable isotopes

The stable isotope results (Table 6) show three groups that can be explained from a geological, hydrological and meteorological point of view. Only one set of samples was taken, so that temporal interpretations are not possible. Firstly, all the nine samples are above the GMWL and the LMWL, the closest complete one for Pretoria, about 300 km west of Bulembu (Fig. 13). This offset is characteristic for monsoon rain influenced water samples, climatic conditions which prevail in the Bulembu area. It has also been shown by Mazor et al. (1974) for the Mkoba river 13 km southeast of Piggs Peak and Piteau Associates Engineering Ltd. (1992) for several rain and spring samples, that these climatic conditions cause lighter isotope samples in eSwatini. Another explanation for that could be the fractionation resulting from the hydration of the silicate minerals, such as feldspars, in the local rocks (Clark and Fritz, 1999). Both $\delta^{18}O$ and $\delta^{2}H$ appear with a low spreading of 0.4 ‰ and 4.2 ‰, respectively, ranging from −4.2 to −3.8 for $\delta^{18}O$ and −17.6 to −13.4 for $\delta^{2}H$. This is also similar to the

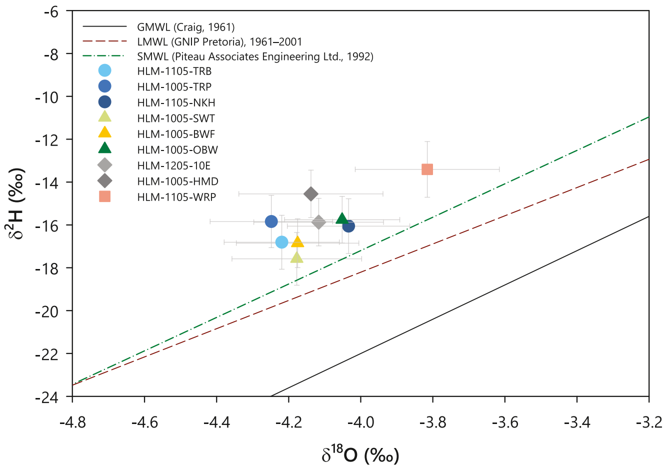

Fig. 13. Stable isotope diagram of the nine water samples taken in May 2023. Symbols and colours identical to those of the Piper diagram. SMWL (Swaziland Meteoric Water Line) taken from Piteau Associates Engineering Ltd. (1992), based on runoff samples. (For interpretation of the references to colour in this figure legend, the reader is referred to the Web version of this article.)

results of Mazor et al. (1974). The heaviest sample, WRP from the waste rock pile, can be attributed to evaporation, which would also explain this sample's higher EC compared to the MIW samples. On the other, heavier end, are the surface water samples that originate in the phyllites of the Onverwacht group, west and southwest of Bulembu. The two mining influenced water samples show slightly heavier isotopic compositions and are in contact with the serpentine ore body. Sample 10E is isotopically close to the surface water sample OBW, which originates in the serpentinite complex east of Bulembu. It seems as if the water flows only a couple of 100 m on the surface after the spring, which due to the area's restricted accessibility, could not be located in the field. The water from sampling location NKH recharges close to the peak of the Emlembe (1862 m), in an altitude of around 1600 m, 500 m above Bulembu, in rocks of the Moodies Group. Without having temporal data available, this sample cannot easily be explained, specifically because it is close to the MIW isotopic composition and the serpentinite samples. Yet, except WRP, all samples show that they did not experience substantial evaporation before they entered the ground or surface water. The stable isotopes can therefore be grouped as follows: surface water samples from an average altitude of 1100–1500 m and the Onverwacht Group, MIW samples from the serpentinite ore body and one evaporation dominated sample from the waste rock pile, with all samples showing monsoon influence.

7.10. Asbestos fibres in the water phase

Asbestos commonly enters the aquatic environment through erosion of rocks, waste materials or asbestos-containing products (e.g. roofing or piping) that have been subjected to weathering, and the US EPA has set the limit for asbestos in drinking water to 7 million particles per liter (Agency for Toxic Substances and Disease Registry, 2001). An additional source of asbestos contamination in water is the deposition of airborne asbestos particles. In the published literature, asbestos has been documented in a wide range of surface and subsurface aquatic environments including naturally occurring asbestos deposits, such as in the Italian Lazio and Balangero areas. Although asbestos minerals undergo a slow dissolution in acid environments, which does not exist in the area of Bulembu, their degradation can be neglected, and they will therefore persist in the aquatic environment for a long time. The primary source of human exposure is outdoor air, with a lesser degree of exposure occurring from indoor air or drinking water (Agency for Toxic Substances and Disease Registry, 2001; Avataneo et al., 2021; IARC Working Group on the Evaluation of Carcinogenic Risks to Humans, 2012). As the drinking water for Bulembu and the nearby En Iembe originates from rocks of the Moodies Series upstream of the mine site, this population will not be affected by water-borne asbestos.

The concentration of fibres in the filtered water samples from location HMD was small, below 10 per 1500 mL of sample, which is far below the limit set by the US EPA. This finding is similar to that of Buzio et al. (2000), who wrote that "the concentration of fibres found … is not at all relevant and worrying for the public health." The reason for those low concentrations is that the mine site is largely undisturbed for more than two decades and most easily transportable fibres were already discharged from the mine. Water samples from tailings run-of could not be taken, as it did not rain during the sampling period. Yet, the local conditions clearly indicate that high fibre concentrations are still transported during intense rainfall. Asbestos fibres can be identified in all the ephemeral water courses leading from the tailings heaps, specifically in the southern direction, towards the Mzilanti valley (Fig. 14). In addition, asbestos can be identified in the riverbed and the banks of the mine discharge and along the river in the Mzilanti valley. Similar conditions in the vicinity of degrading mine installations have been described from the abandoned Uitkyk and Lagerdraai asbestos mines in Limpopo, South Africa (Freemantle et al., 2022). Because waterborne asbestos can enter the air (Avataneo et al., 2022), it is essential that the redeposition of asbestos from abandoned structures or the tailings is kept to a minimum, for example by tailings amelioration (e.g. Mitchell et al., 1991).

7.11. Tracer tests

Three tracer tests were conducted at the mine site. The only known location, where the MIW discharges is the drainage gallery that ends in the Mzilanti valley south of Bulembu (HMD). No increase in EC was observed within four days of injection of the **sodium chloride** tracer, possibly because the high-density salt had sunk to deeper parts of the shaft and the sampling time was too short. In contrast, the **uranine** tracer could be detected already 1–1.5 days after injection at a flow rate of around 3266 L/min at HMD and the recovery rate was 73% after 38 days, when the 2023 uranine tracer test was ended and 100 % after 20 days, when the logger's battery went flat during the 2024 test (Fig. 15). Based on the sum curves, the mean residence time of the tracer was 8–9 days and the peak concentration after 3–4 days. No **Eosin Y** tracer could be detected at HMD, which either due to a too short tracer test duration or a missing connection between 10E and HMD. These tracer test data show that there is a good hydraulic connection between locations HVS and HMD, and the mean residence time of the MIW close to the surface of the mine pool seems to be short and possibly well mixed. This explains the relatively low mineralisation compared to the water draining through the Bulembu waste rock pile and the similar water quality at the drainage adit and the incline (location 10E). Because there is no direct connection between the vertical shaft and the drainage adit, it is not clear, how exactly the water flows from the injection location on the water surface (level 155). Based on information from a former mine worker, inclines connected the 155 level to the water outlet back in 1970–1980, but since ore extraction broke the stopes, workings and mine voids, water very likely flows today through or percolates the broken rock (pers. comm. Phil Wikberg 2023) from the shaft to the discharge adit. This would explain the two tracer peaks in the breakthrough curve.

Three days after injection, tracer concentrations in the vertical shaft exhibited a range of values between 26 and 34 μg/L. These concentrations were relatively constant up to a water depth of 72 m (5 level), indicating convective transport. From there, they increased steadily to 34 μg/L at a depth of 335 m (7 level), indicative of diffusive transport. The interpolation of the tracer concentration to the shaft sump yielded a result of 0.51 g of the 1000 g of injected uranine that was still present in the shaft three days after tracer injection. This provides evidence that the tracer recovery rate of 100% at HMD is accurate.

Fig. 14. Eroded asbestos tailings south of Bulembu. Right image is detail, showing the cm high earth pyramids with asbestos fibre that will be eroded by rainfall events (width ≈ 1 m).

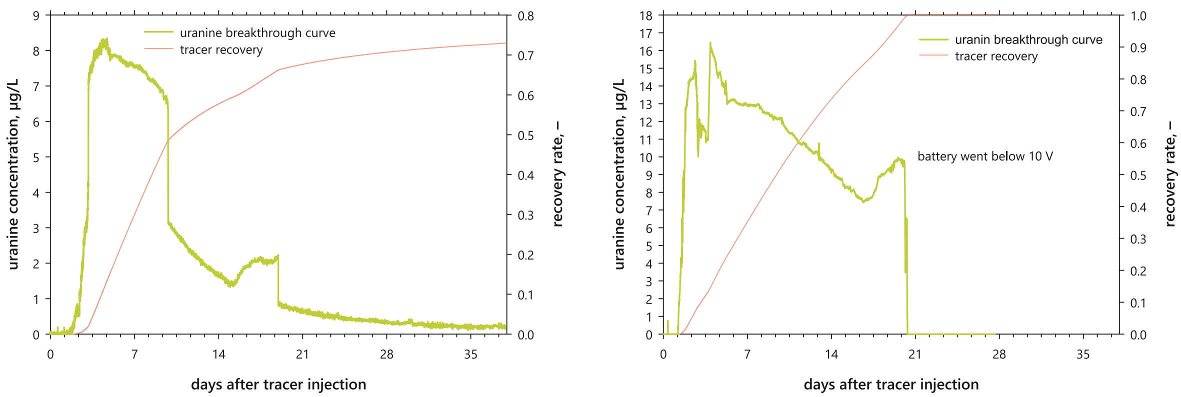

Fig. 15. Uranine breakthrough and tracer recovery curve of the May 2023 (left, ≈500 g) and February 2024 (right, ≈1000 g) tracer tests. First tracer arrival after 1–1.5 days and mean residence time 8–9 days.

7.12. Camera logs and shaft logging

Camera logs were conducted in all the four compartments of the Havelock vertical shaft. Two of them (NE and SE) are blocked by a wire mesh in 99.9 m (3 level) and another one (SW) at 341.8 m (7 level) below shaft collar. The last one (NW) is the ladder compartment and is accessible down to 8.3 m. These beforementioned wire meshes were used to separate the four compartments and fell into the shaft as soon as their stability deteriorated, or they were damaged when the miners cut of the hoisting cage which could be deduced from the traces of hoisting rope in the same depth. As a result, a full EC–temperature log could not be taken. What could be seen was that water was dropping down the shaft below a depth of ≈35 m, very likely coming from drainage cementation holes into and through the shaft lining (pers. comm. Phil Wikberg 2023) and there was a lot of dust in the open space above that depth. From the December 2022 and February 2024 investigations it is known that the water level is at a depth of 106.9–107.3 m below the shaft collar corresponding with the elevation of the mine water discharge at HMD.

Multiparameter measurements in the SW compartment down to a depth of 183 m showed that the temperature is around 20.8 °C with fluctuations characteristic for turbulent convective flow above 5 level and possibly diffusive flow below 5 level. pH steadily decreases from 8.6 to 8.5, a trend, which was also observed in some flooded shafts of the Wismut uranium mine in Germany (Wolkersdorfer, 1996). Electrical conductivity is 342.3 µS/cm above 5 level and 343.5 µS/cm below, with a high fluctuation. The speed of sound constantly increases from 1484,9 m/s to 1488.0 m/s with fluctuations on 5 level and the 3 level loading station. These measurement show that the water from the vertical shaft flows downward from level 3 to level 5 and from there via various galleries and working levels to the discharge location.

7.13. BART tests

Results of the BART tests were not conclusive, possibly because the vials fell over during the transport, or the tests were past their three-year shelf live. Only the Sulfate-reducing Bacteria (SRB) and Slime-forming Bacteria (SLYM) samples from the waste rock pile showed a high aggressivity with 910 pac/mL (predictive active cells) and 632 thousand pac/mL, respectively. SRB results from the Bulembu waterfall (BWF) showed no Sulfate-reducing Bacteria. All the other four samples could not be utilized.

8. Discussion

Based on the results of this study, the water samples around Bulembu and the abandoned Havelock mine can be categorised into mine uninfluenced water, mining influenced water and waste rock pile water. They differ substantially in their chemical and physico-chemical parameters, reflecting their individual residence time and evolution. With the data collected and the numerical modelling, it was not possible to attribute any particular sample to a specific rock formation around Bulembu, although the Onverwacht Group samples have slightly lower TDS concentrations than those from the Moodies Group. Yet, when plotting the molar concentrations of Mg and Ca vs. the EC, the three groups described earlier can be identified as belonging to the mica schists and the serpentine lithologies (Fig. 8). All surface waters show very low mineralisation with circumneutral pH-values, while the MIW is characterised by higher pH values between 8.1 and 9.0. The surface water samples meet WHO drinking water standards for inorganic parameters, while the waste rock samples have Cr concentrations, and the mine pool samples have As concentrations above WHO standards. None of the water samples developed acidic conditions, as has also been shown by Meck et al. (2006) for abandoned Zimbabwean asbestos mines. It can therefore be concluded that the hydrochemical characteristics of the water in and around Bulembu are of exceptionally good quality.

The mean residence time of the mine pool water is low, as indicated by the tracer test results (8–9 days) and the low TDS concentrations. In addition, the mine pool water appears to be well mixed, as evidenced by the similar chemical composition of the water at the discharge adit and the incline in the eastern part of the mine. The quality of the MIW may be mainly due to the 22-year flushing period and the fact that the first flush is in the final phase. The water seeping into the mine also appears to be of very good quality, as shown by sample 1EA, which contributes around 8% to the flow rate of the MIW.

The current course of the Tutusi River, which originates in the rocks of the Onverwacht Group, is a result of its diversion during mining activities. Instead of flowing south, it now flows east into the Nkomazana river. This affects the chemical composition of the Tutusi River water which can be seen at sampling points TRB before the diversion and TRP after the diversion. A mixing calculation of the TRB and OBW waters showed that the river water, which originates from Onverwacht Group rocks south of the summit, is influenced by serpentinite and Moodies Group waters at OBW. A mixing ratio of 3:7 OBW to TRB water gives a chemical composition of the TRP water. This is also reflected in the stable isotopes by a trend towards the heavier δ^2H composition and in the species distribution by a distinction between TRB and TRP water. It indicates that the Tutusi River, between the outflow from the diversion tunnel and the confluence with the Nkomazana river, is influenced by water from the hilly serpentinite outcrops of the Moodies Group, east of Bulembu.

The proposed re-mining of the Havelock asbestos tailings by Kobolondo Magnesium (Salamander Magnesium International, Mauritius) will involve the reprocessing of the asbestos-containing serpentinite, resulting in the redistribution of asbestos fibres into the air and water (Salamander Mining, 2020). This will affect not only the miners, but also the orphanage children, workers and residents, as well as animals like monkeys, now living on the mine site. Negative effects of asbestos mining on the local population at Havelock have been described by McCulloch (2003), who found at least two cases of asbestosis with wives of former miners. He writes that the asbestos that caused these women's disease, and who had no occupational exposure, might have come either from the mill's dust, the asbestos tailings or the waste rock dumps around the mine.

9. Conclusions

With regard to asbestos from the Havelock mine, the good water quality observed is not necessarily guaranteed everywhere, as a good chemical water quality does not mean that the water is free of asbestos, as the results of this study show. Avataneo et al. (2022) pointed out that the dangers of waterborne asbestos have been underestimated so far. They were able to show that elevated concentrations of asbestos in water can be released to the atmosphere by water-to-air migration, and therefore care should be taken not to contaminate groundwater or surface water with redistributed asbestos, for example from tailings processing. In addition, the concentration of fibres in the water phase will increase should remining start, leaving negative effects on downstream users, as described by Mhlanga-Mdluli (2012) in relation to trout in the Komati River.

Bearing in mind that Bulembu and the abandoned Havelock mine are directly adjacent to the Barberton Makhonjwa Mountains UNESCO World Heritage Site and that geotourism represents an increasingly popular sector in the tourism market (Grobbelaar et al., 2019; Schlüter and Schumann, 2018), the authors conclude that the optimal management of the Bulembu and Havelock region would be to incorporate the area into a transboundary national park with further development of tourism to support the local community and the Bulembu Ministries. This would ensure that the prestigious nature and the currently very good water quality of the rivers around Bulembu would be maintained in the future. It would also allow to create funds for the total or partial cover of the waste rock pile and installation of a passive mine water treatment system (which would also lower the number of asbestos fibres in the MIW) downstream the Havelock mine discharge location.

Funding sources

Christian Wolkersdorfer – NRF Grant UID 86948.
Elke Mugova – Forum Bergbau und Wasser (Germany)
Nokuthula Nchabeleng – NRF (Ref Number CSRP2204204025) and TIA (Ref Number 13971/01)

Disclose of AI-assisted technologies

During the preparation of this work the authors used deepl.com/write to improve the English writing. In some cases, the authors used ChatGPT 3.5 or 4o to language improve individual sentences or small paragraphs. After using these tools, the authors reviewed and edited the content as needed and take full responsibility for the content of the publication.

CRediT authorship contribution statement

Christian Wolkersdorfer: Writing – review & editing, Writing – original draft, Investigation, Funding acquisition. **Kagiso S. More:** Writing – original draft, Investigation. **Elke Mugova:** Writing – review & editing, Writing – original draft, Investigation. **Nokuthula Nchabeleng:** Writing – original draft, Investigation. **Anna Johanna Sotiralis:** Writing – original draft, Investigation.

Declaration of competing interest

The authors declare that they have no known competing financial interests or personal relationships that could have appeared to influence the work reported in this paper.

Acknowledgements

The authors thank Kurt Puttkammer, Klaus Schiller, Richard Tucker and Sicelimphilo Dludlu from the Bulembu Ministries (eSwatini), for their support in conducting the research in Bulembu. Special thanks to Owen Buchanan for sharing his local knowledge and providing his weather station data as well as Colani Maziya for assisting in sampling and guiding us to "unreachable" sampling locations. Phil Wikberg, Ben Scholten, Darrun Raw and Michael Simelane contributed with their knowledge of the Havelock mine. We also thank the following descendants of Havelock mine workers, who provided insights: Albert Ntimane, Tammy Dlamini, Mpumelelo Shabangu but specifically Cebsile Thwala and Mpumelelo Shabangu who reported about their fathers' asbestosis cases. Funding was provided by Tshwane University of Technology's (TUT) Mine Water Chair (NRF Grant UID 86948) and the University of Pretoria's (UP) Water Utilisation and Environmental Engineering Group (NRF CSRP2204204025 and TIA 13971/01). Swaziland vector images are from Free Vector Maps.

Appendix A. Supplementary data

Supplementary data to this article can be found online at https://doi.org/10.1016/j.jafrearsci.2024.105533.

Data availability

Data will be made available on request.

References

Agency for Toxic Substances and Disease Registry, 2001. Toxicological Profile for Asbestos. U. S. Department of Health & Human Services, Atlanta, p. 327.

Anhaeusser, C.R., 1976. The nature of chrysotile asbestos occurrences in southern Africa – a review. Econ. Geol. 71, 96–116.

Anhaeusser, C.R., 1986. The geological setting of chrysotile asbestos occurrences in Southern Africa. In: Anhaeusser, C.R., Maske, S. (Eds.), Mineral Deposits of Southern Africa. Geol. Soc. S. Afr., pp. 359–375. Johannesburg, South Africa, South Africa.

Anonymous, 1978. Havelock asbestos mine. Swaziland Today September 1978, 35–36.

Appelo, C.A.J., Groen, M.M.A., Heidweiller, V.M.L., Smit, P.M.H., 1983. Hydrochemistry of springs in an alpine carbonate/serpentinite terrain. Int. Conf. Water-Rock Interaction, Misasa, Japan 26–31.

Avataneo, C., Belluso, E., Capella, S., Cocca, D., Lasagna, M., Pigozzi, G., De Luca, D.A., 2021. Groundwater asbestos pollution from naturally occurring asbestos (NOA) – a preliminary study on the Lazio valleys and Balangero plain area, NW Italy. Ital. J. Eng. Geol. Environ. Special Issue 5–19.

Avataneo, C., Capella, S., Luiso, M., Marangoni, G., Lasagna, M., De Luca, D.A., Bergamini, M., Belluso, E., Turci, F., 2023. Waterborne asbestos: good practices for surface waters analyses. Front. Chem. 11, 1104569.

Avataneo, C., Petriglieri, J.R., Capella, S., Tomatis, M., Luiso, M., Marangoni, G., Lazzari, E., Tinazzi, S., Lasagna, M., De Luca, D.A., Bergamini, M., Belluso, E., Turci, F., 2022. Chrysotile asbestos migration in air from contaminated water: an experimental simulation. J. Hazard Mater. 424, 127528.

Baron, P.A., 2016. Measurement of Fibers, NIOSH Manual of Analytical Methods (NMAM), 5th ed. NIOSH, Cincinnati, pp. FI-1–FI-31.

Barton, C.M., 1986. The Havelock asbestos deposit in Swaziland, Barberton greenstone belt. In: Anhaeusser, C.R., Maske, S. (Eds.), Mineral Deposits of Southern Africa. Geol. Soc. S. Afr., Johannesburg, pp. 395–407.

Bartrip, P.W.J., 2000. Nellie Kershaw, Turner and Newall, and asbestos-related disease in 1920s Britain. Hist. Stud. Ind. Relat. 2000, 101–116.

Bartrip, P.W.J., 2001. The Way from Dusty Death – Turner and Newall and the Regulation of the British Asbestos Industry, 1890s–1970. The Athlone Press, London.

Buzio, S., Pesando, G., Zuppi, G.M., 2000. Hydrogeological study on the presence of asbestos fibres in water of northern Italy. Water Res. 34, 1817–1822.

Cairncross, B., 2022. Minerals & gemstones of Southern Africa. Struik Nature, Century City, p. 320.

Clark, I.D., Fritz, P., 1999. Environmental Isotopes in Hydrogeology, 2nd print ed. Lewis, Boca Raton.

Coakley, G.J., 2001. Minerals Yearbook – the Mineral Industry of Swaziland, U.S. Geological Survey Minerals Yearbook—2001. U.S. Geol Survey, Reston, pp. 27.21–27.23.

Cornelissen, H., Watson, I., Adam, E., Malefetse, T., 2019. Challenges and strategies of abandoned mine rehabilitation in South Africa: the case of asbestos mine rehabilitation. J. Geochem. Explor. 205, 106354.

Cullimore, D.R., 1999. Microbiology of Well Biofouling. Lewis, Boca Raton.

de Villiers, S., de Wit, M.J., 2007. Sources of river water radiogenic strontium: examples from the Achaean granite dominated catchments of Swaziland. S. Afr. J. Geol. 110, 349–366.

Dean, R.M., 1978. Mining in the Southern Africa Region, A Report to the Congress on Development Needs and Opportunities for Cooperation in Southern Africa – Annex B Mining. United States Agency for International Development, Washington,, p. 57.

Flanagan, D.M., 2023. Asbestos. U.S. Geological Survey, Mineral Commodity Summaries 1–2.

Freemantle, G.G., Chetty, D., Olifant, M., Masikhwa, S., 2022. Assessment of asbestos contamination in soils at rehabilitated and abandoned mine sites, Limpopo Province, South Africa. J. Hazard Mater. 429, 127588.

Furtak, H., Langguth, H.R., 1967. Zur hydrochemischen Kennzeichnung von Grundwässern und Grundwassertypen mittels Kennzahlen [Hydrochemical characterisation of groundwater and groundwater types using indicator numbers]. Mem. IAH-Congress 7, 86–96, 1965.

Gan, S., Birrell, L., Robbertze, D., Zhao, B., van Niekerk, E., Ncubi, L., 2022. Quality control in tailings resource exploration at Havelock Mine. Eswatini. J. S. Afr. I. Min. Metall. 122, 1–16.

Government of eSwatini, 2018. Eswatini National Water Policy, 2018.

Government of Swaziland, 2000. Water Bill, 2000 – Bill No. 7 of 2000, vol. 38. Swaziland Government Gazette – Supplement, pp. S1–S44.

Grobbelaar, L., Bouwer, S., Hermann, U.P., 2019. An exploratory investigation of visitor motivations to the Barberton – Makhonjwa geotrail, South Africa. GeoJournal of Tourism and Geosites 25, 283–292.

Hall, A.L., 1918. The geology of the Barberton gold mining district including adjoining portions of northern Swaziland. Mem. S. Afr. Geol. Surv. 9, 1–347.

Hall, A.L., 1930. Asbestos in the Union of South Africa (2nd edn). Mem. S. Afr. Geol. Surv. 12, 1–324.

Hall, A.L., 1931. The Havelock asbestos mine. S. Afr. Mining. Eng. J. 42, 85–87.

Hem, J.D., 1985. Study and interpretation of the chemical characteristics of natural water. U. S. Geol. Surv. Water Supply Pap. 2254, 263.

Hofmann, A., Anhaeusser, C.R., Li, X.H., 2021. Layered ultramafic complexes of the Barberton Greenstone Belt – age constraints and tectonic implications. S. Afr. J. Geol. 124, 7–16.

IARC Working Group on the Evaluation of Carcinogenic Risks to Humans, 2012. A Review of Human Carcinogens. Part C: Arsenic, Metals, Fibres, and Dusts. IARC Monographs, 100C, pp. 1–501.

John, T., 2020. Grassroots literacy and the written record – a textual history of asbestos activism in South Africa. Multilingual Matters,. Bristol, 00002.

Johnson, M.R., Anhaeusser, C.R., Thomas, R.J., 2006. The Geology of South Africa. Council for Geoscience, Pretoria.

Jourdan, P., 1990. The minerals industry of Swaziland. IMR Open Rep. Inst. Min. Res. 104, 1–8.

Kazan-Allen, L., 2003. Asbestos abroad – an international Overview. British Asbestos Newsletter 51, 1–17.

Langmuir, D., 1997. Aqueous Environmental Geochemistry. Prentice Hall,. Upper Sadle River.

Mazor, E., Verhagen, B.T., Negreanu, E., 1974. Hot Springs of the Igneous Terrain of Swaziland – Their noble gases, hydrogen, oxygen and carbon isotopes and dissolved ions. In: International Atomic Energy Agency (Ed.), Isotope Techniques in Groundwater Hydrology 1974. International Atomic Energy Agency, Vienna, pp. 29-47.

McCulloch, J., 2003. Asbestos Mining and Occupational Disease in Southern Rhodesia/Zimbabwe, 1915–98. Hist. Workshop J. 2003, pp. 131–152.

McCulloch, J., 2005. Dust, disease and labour at Havelock asbestos mine, Swaziland. J. South Afr. Stud. 31, 251–266.

McCulloch, J., Miller, P., 2023. Things fall apart – independent research, asbestos litigation and the gold miners' class action: 1983–2019. In: McCulloch, J., Miller, P. (Eds.), Mining Gold and Manufacturing Ignorance: Occupational Lung Disease and the Buying and Selling of Labour in Southern Africa. Palgrave Macmillan, Singapore, pp. 371–402.

McCulloch, J., Tweedale, G., 2008. Defending the Indefensible – the Global Asbestos Industry and its Fight for Survival. Oxford University Press, Oxford.

McDermott, M., Bevan, M.M., Elmes, P.C., Allardice, J.T., Bradley, A.C., 1982. Lung function and radiographic change in chrysotile workers in Swaziland. Br. J. Ind. Med. 39, 338–343.

Meck, M., Love, D., Mapani, B., 2006. Zimbabwean mine dumps and their impacts on river water quality – a reconnaissance study. Phys. Chem. Earth 31, 797–803.

Merewether, E.R.A., Price, C.W., 1930. Report on effects of asbestos dust on the lungs and dust suppression in the asbestos industry – Part I. Occurrence of pulmonary fibrosis and other pulmonary affections in asbestos workers – Part II. Processes giving rise to dust and methods for its suppression. H.M. Stationery Off.,London, 34.

Mhlanga-Mdluli, P.P., 2012. Anthropogenic pollution of the Lusushwana river at Matsapha, and prospects for its control: Kingdom of Swaziland (eSwatini). Department of Civil & Building Engineering. Loughborough University, Loughborough, p. 342.

Mitchell, P.B., Waller, C.P., Atkinson, K., Edvards, R.P., 1991. Ameliorative techniques in improving revegetation schemes. Proceedings, 4th International Mine Water Association Congress 2, 281–293.

Mlilo, P., Mhlanga, N.B., Senzanje, A., 2008. Emerging issues in water Resources management in Swaziland. 12th Biennial Conference of the International Association for the Study of the Commons, pp. 1–15. Cheltenham.

Moerdyk, C., 1943. Swaziland Havelock Mine. Inspector of Mines, Pretoria, 2/6/1943, p. 62.

Parkhurst, D.L., Appelo, C.A.J., 2013. Description of input and examples for PHREEQC version 3 – a computer program for speciation, batch-reaction, one-dimensional transport, and inverse geochemical calculations. U.S. Geol. Surv. Tech. Methods 6, 1–497.

Phillips, J.I., Rees, D., Murray, J., Davies, J.C.A., 2012. Mineralogy and malignant mesothelioma: the South African experience. In: Belli, C., Anand, S. (Eds.), Malignant Mesothelioma. IntechOpen, London, pp. 1–30.

Pim, A.W., 1932. Commission appointed by the secretary of state for dominion affairs. Financial and Economic Situation of Swaziland. H.M. Stationery Off., London.

Piper, A.M., 1944. A graphic procedure in the geochemical interpretation of water analyses. Trans. Am. Geophys. Union 25, 914–923.

Piper, A.M., 1953. A graphic procedure in the geochemical interpretation of water analyses. U.S. Geol. Surv. Ground Water Notes Geochem. 12, 1–14.

Piteau Associates Engineering Ltd., 1992. Groundwater Resources of Swaziland. Government of Swaziland – Department of Geological Surveys and Mines & Canadian International Development Agency, North Vancouver, p. 55.

Pohl, W., 2020. Economic Geology – Principles and Practice, second ed. Schweizerbart, Stuttgart.

Ross, M., 1981. The geologic occurrences and health hazards of amphibole and serpentine asbestos. In: Veblen, D.R., Ribbe, P.H. (Eds.), Amphiboles and other Hydrous Pyriboles. De Gruyter, Berlin, pp. 279–324.

Ross, M., 1999. The health effects of mineral dusts. In: Plumlee, G.S., Logsdon, M.J. (Eds.), The Environmental Geochemistry of Mineral Deposits. Society of Economic Geologists, Littleton, pp. 339–356.

Sacchi, E., Bergamini, M., Lazzari, E., Musacchio, A., Mor, J.R., Pugliaro, E., 2021. Natural background levels of potentially toxic elements in groundwater from a former asbestos mine in serpentinite (Balangero, north Italy). Water 13, 735.

Salamander, Mining, 2020. The Kobolondo Project – Unlocking Resource Value for Eswatini. Salamander Mining, Mauritius, p. 7.

Schapira, J.S., Bolhar, R., Master, S., Wilson, A.H., 2023. Mineralogical, petrological and geochemical characterisation of chrysotile, amosite and crocidolite asbestos mine waste from southern Africa in context of risk assessment and rehabilitation. Minerals 13, 1352.

Schlüter, T., Schumann, A., 2018. Geosites as a potential for the development of tourism – Overview of relevant sites in eswatini (formerly Swaziland). GeoJ. Tour. Geosites 22, 535–547.

Scott, P., 1950. Mineral development in Swaziland. Econ. Geogr. 26, 196–213.
Scott, R.L., Hays, R.M., 1975. Inactive and Abandoned Underground Mines – Water Pollution Prevention and Control. U.S. Environmental Protection Agency, Washington.
Slade, G.F.M., 1930. The Incidence of Respiratory Disability in Workers Employed in Asbestos Mining, with Special Reference to the Type of Disability Caused by the Inhalation of Asbestos Dust. Univ. of the Witwatersrand, p. 150 unpublished.
Swaziland Ministry of Commerce Industry and Mines, 1970. Annual Report of the Geological Survey and Mines Department for the Year Ending 31st December 1970, Mbabane, p. 32.
Thives, L.P., Ghisi, E., Thives Júnior, J.J., Vieira, A.S., 2022. Is asbestos still a problem in the world? A current review. J. Environ. Manag. 319, 115716.
Tweedale, G., 2001. Magic Mineral to Killer Dust – Turner & Newall and the Asbestos Hazard. Oxford University Press, Oxford.
UN Department of Technical Cooperation for Development, 1989. Swaziland, Ground Water in Eastern, Central and Southern Africa. United Nations, New York, pp. 260–268.
UNESCO, 2018. Decision 42 COM 8B.5 – Barberton Makhonjwa Mountains (South Africa). In: WHC/18/42.COM/18. UNESCO World Heritage Centre, Manama, pp. 182–185.
Vallero, D.A., Blight, G., 2019. Mine waste: a brief Overview of origins, quantities, and methods of storage. In: Letcher, T.M., Vallero, D.A. (Eds.), Waste – A Handbook for Management, second ed. Academic Press, San Diego, pp. 129–151.
van Biljon, W.J., 1959. The Nature and Origin of the Chrysotile Asbestos Deposits in Swaziland and the Eastern Transvaal. University of the Witwatersrand, Johannesburg, p. 130.
Wagner, J.C., 1963. Asbestosis in experimental animals. Br. J. Ind. Med. 20, 1–12.
Ward, J.H.W., 1995. Geology and metallogeny of the Barberton greenstone belt: a survey. J. Afr. Earth Sci. 21, 213–240.
Wolkersdorfer, C., 1996. Hydrogeochemische Verhältnisse im Flutungswasser eines Uranbergwerks – Die Lagerstätte Niederschlema/Alberoda. Clausthal. Geowiss. Diss. 50, 1–216.
Wolkersdorfer, C., 2008. Water management at abandoned flooded underground mines – fundamentals, tracer tests, modelling. Water Treatment. Springer, Heidelberg.
World Health Organization (WHO), 2017. Guidelines for Drinking-Water Quality, fourth ed. World Health Organization, Geneva.
Wrucke, C.T., 1995. Serpentine- and Carbonate-Hosted Asbestos Deposits (Models 8d, 18e; Page, 1986; Wrucke and Shride, 1986). In: du Bray, E.A. (Ed.), Preliminary Compilation of Descriptive Geoenvironmental Mineral Deposit Models. U.S. Geological Survey, Denver, pp. 39–46.
Yu, M.-H., Tsunoda, H., Tsunoda, M., 2012. Environmental Toxicology – Biological and Health Effects of Pollutants, third ed. CRC Press, Boca Raton.
Zaidi, S.H., Shanker, R., Dogra, R.K.S., 1973. Experimental infective pneumoconiosis: effect of asbestos dust and *Candida albicans* infection on the lungs of rhesus monkeys. Environ. Res. 6, 274–286.